renal failure patients as well as the healthy subjects because the covalent protein-binding formation between HSA and thiol-containing drug, Bucillamine, increased in several pathological states, such as renal failure, diabetes, hepatitis, and rheumatism.[6]

Methods

Materials: HSA was purchased from Chemo-Sero-Therapeutic Research Institute (Kumamoto, Japan) or purified from human serum. Purification of albumin from human serum was performed according to the method of Watanabe *et al.*[7] Briefly, serum was applied to a Blue Sepharose affinity chromatography column, which was pre-treated with 0.2 M sodium acetate (pH 5.5). The column was then washed with 0.2 M sodium acetate (pH 5.5) and 1 N sodium chloride, and albumin was eluted with 0.02 M sodium acetate and 3 M sodium chloride (pH 6.5). The albumin containing fraction was dialyzed against water, freeze-dried, and de-fatted. Purification of albumin was confirmed by SDS-PAGE and Western blotting.

NAC was purchased from Sigma Chemical Co. (St. Louis, MO, USA). N-acetyl-L-[1-^{14}C] cysteine (^{14}C-NAC) was synthesized by Amersham Pharmacia Biotech Ltd. (Buckinghamshire, UK) and was purified before use. The radiochemical purity was >95% and the specific radioactivity was 2.15 MBq/μmol NAC. All other chemicals or solvents were of analytical or HPLC grade.

Human serum: The protocol used in this study followed the tenets of the Declaration of Helsinki promulgated in 1964 and was approved by the institutional review board and informed consent was obtained from all subjects. Five stable hemodialysis patients (3 men and 2 women) aged 71 to 77 years, of dialysis age ranging from 5 to 9 years, were enrolled in the study. Five gender-matched healthy subjects were also investigated as a control group. End-stage renal failure was the result of glomerulonephritis (n = 5).

HPLC conditions: The HPLC system comprised an LC-4A pump (Shimadzu, Tokyo, Japan) equipped with a gradient programmer and a Shimadzu SPD-2AS ultraviolet (UV) monitor. The column packing material, *N*-methylpyridinium polymer cross-linked with ethylene glycol dimethacrylate (4VP-EG-Me), was prepared as described previously.[8] HSA was eluted using a 30-min linear gradient of 0 to 0.5 M sodium chloride in 0.05 M Tris-AcOH buffer (pH 6.5) at a flow rate of 0.5 mL/min at 25°C and the detection wavelength was 280 nm.

Definition of HSA: HSA can be classified into two main sub-types; mercaptoalbumin and nonmercaptoalbumin (**Fig. 1**). These sub-types are referred to as HMA and HNA, respectively. Although HNA is a general term that includes both the L-cysteine (Cys)-bound type and the oxidized type, HSA-Cys disulfide and oxidized

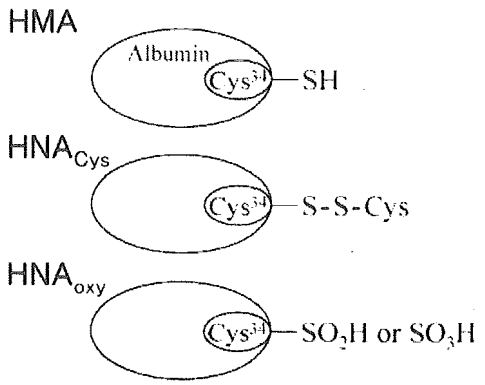

Fig. 1. Illustrations showing intrinsic HSA sub-types classified by the structure of the Cys^{34} moiety. HMA: human mercaptoalbumin. HNA: human nonmercaptoalbumin.

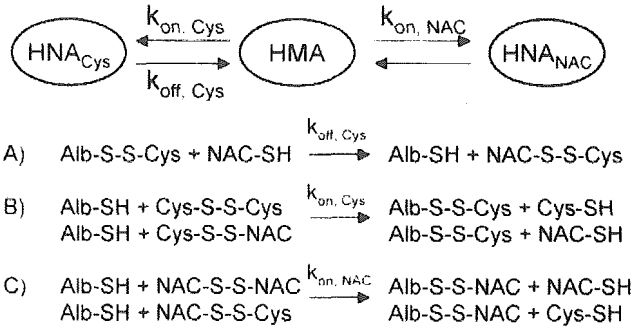

Fig. 2. Diagram showing the conversion of HSA among its sub-types through a thiol-disulfide exchange reaction when NAC is added and its kinetic model.

HSA are referred to as HNA_{Cys} and HNA_{oxy}, respectively in this study (**Fig. 1**).

Assay conditions: HSA was dissolved in phosphate buffer (pH 7.4, 0.067 M, $\mu = 0.15$) from which endogenous oxygen had previously been removed by sonication and nitrogen replacement. The HSA solution (approximately 300 μM) was preincubated at 37°C for 5 min and then approximately 1500 μM NAC was added. The mixture was incubated at 37°C under anaerobic conditions. Aliquots were analyzed by HPLC at various incubation times.

For analysis of HSA incubated with ^{14}C-labelled NAC, column eluent was collected at 30-second intervals and the radioactivity of each fraction were determined.

Calculation of kinetic parameters: The reaction between HSA and low-molecular thiol-compounds was expected to proceed through the thiol-disulfide exchange reaction. Possible mechanisms of the interactions between HSA, NAC, and Cys, which is the most abundant thiol-compound retained by HSA, are shown in **Fig. 2**. The kinetic parameters $k_{off,Cys}$, $k_{on,Cys}$, and $k_{on,NAC}$ were defined as the apparent first-order rate constants, representing the dissociation of Cys from HNA_{Cys}, the

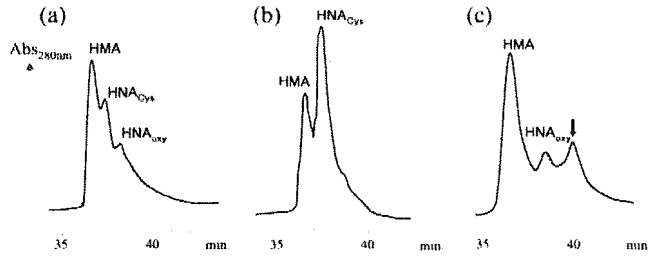

Fig. 3. UV chromatogram of HSA after application to the 4VP-EG-Me column. (a) HSA from healthy volunteer. (b) HSA from renal failure patient. (c) HSA from healthy volunteer incubated with NAC at 37°C for 48 h. Assay conditions are described in the Materials and Methods section.

binding of Cys to HMA, and the binding of NAC to HMA, respectively. These parameters were obtained as follows.

The concentrations of each sub-type of HSA were indicated as a percentage of each chromatographic peak against the total HSA peak area. The common logarithms of the concentrations were plotted against the incubation time and then correlation lines were obtained by the least-squares method. The slopes of these lines correspond to the rate constants (h^{-1}) for the reactions.

Results

HPLC chromatogram of HSA: HSA was primarily separated into three sub-types (in order of abundance; HMA, HNA_{Cys}, and HNA_{oxy}) on the 4VP-EG-Me column chromatography (**Fig. 3**). The ratio of three sub-types ($HMA:HNA_{Cys}:HNA_{oxy}$) in HSA from healthy subjects was approximately 5:4:1 (**Fig. 3(a)**). On the other hand, HSA from renal failure subjects showed an extreme decrease in HMA and an increase in HNA_{Cys} (**Fig. 3(b)**).

Following incubation of HSA with NAC at 37°C, the HNA_{Cys} peak was almost disappeared and a new peak was formed behind the HNA_{oxy} peak (**Fig. 3(c)**). When incubated with ^{14}C-labelled NAC, the radioactive peak corresponded to the newly formed peak (**Fig. 4**), thus suggesting that the newly formed peak corresponded to the stable complex of HSA and NAC, i.e., HSA-NAC mixed disulfide (HNA_{NAC}).

Time-courses of each HSA sub-type after incubation with NAC: **Figure 5** shows the time-concentration plots of each albumin sub-type (HMA, HNA_{Cys}, HNA_{oxy}, and HNA_{NAC}) after incubation of healthy HSA with NAC. During the 2 hours from the start of incubation, HNA_{Cys} rapidly decreased and HMA increased in a complementary manner, and this was followed by a slow reversal, with HNA_{Cys} and HMA increasing and decreasing, respectively. These changes suggest that HNA_{Cys} was rapidly divided into HMA and free Cys by NAC during the first stage of incubation, and Cys then

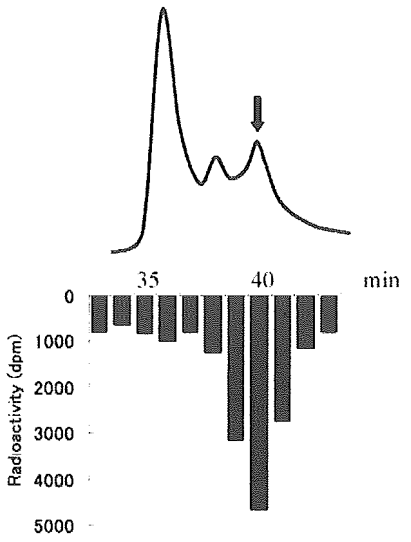

Fig. 4. UV chromatogram and radioactivity distribution of column eluent fractions after HSA was incubated with ^{14}C-labelled NAC for 48 h.

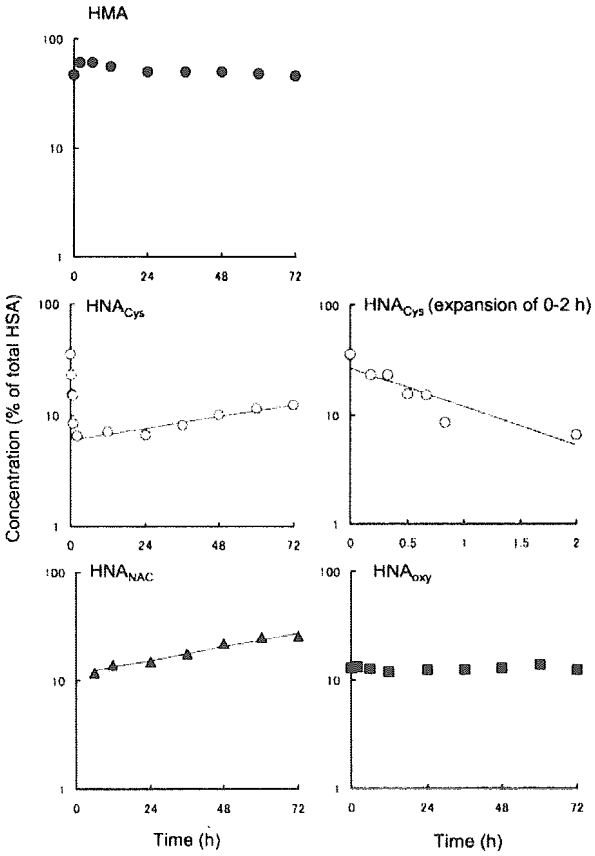

Fig. 5. Time-concentration plots of HSA sub-types after incubation with NAC. Concentrations are indicated as the percentage of each sub-type against the total HSA detected as chromatographic peak area. In the case of HNA_{Cys}, the short time range (0 ~ 2 h) was expanded as a separate figure. Each solid line indicates the correlation obtained by the least-squares method.

Table 1. Binding and dissociation rate constants of covalent binding between HSA and NAC or Cys obtained by adding NAC to HSA.

HSA source	Rate constant (h^{-1})		
	$k_{off,Cys}$	$k_{on,Cys}$	$k_{on,NAC}$
Commercial[a]	1.30	0.00107	0.00330
Healthy volunteers[b]	1.31 ± 0.09	0.000835 ± 0.000298	0.00323 ± 0.00037
Renal failure patients[b]	0.448 ± 0.059	0.000765 ± 0.000271	0.00941 ± 0.00276

[a] Purchased from Chemo-Sero Therapeutic Research Institute.
[b] Purified from sera in our laboratory. Data of HSA purified from sera are represented as mean ± SD (n = 5).

slowly re-bound to HSA. On the other hand, the binding of NAC to HSA, i.e., the formation of HNA_{NAC}, was only detectable after 6 hours incubation. The formation of HNA_{NAC} was as slow as the re-binding of Cys to HSA. HNA_{oxy} was unchanged throughout the incubation period.

Kinetic parameters of protein-binding: Table 1 shows the binding and dissociation rate constants between either HSA and Cys or HSA and NAC. The binding rate constant of Cys to HSA ($k_{on,Cys}$) was approximately 0.001 (h^{-1}) whether the used HSA was commercially obtained or purified from the serum of healthy subjects or dialysis patients. On the other hand, the binding rate constant of NAC to commercial HSA and healthy HSA ($k_{on,NAC}$) was approximately 0.003 (h^{-1}), but the rate was greater in the dialysis patient HSA (approximately 0.01 (h^{-1})). In contrast to these relatively low values, the dissociation rate constant of Cys from HSA ($k_{off,Cys}$) was much greater in the commercial and healthy HSA (1.3 (h^{-1})) as well as in the dialysis patient HSA (0.45 (h^{-1})).

Discussion

The strong anion-exchange polymer *N*-methyl-pyridinium (4VP-EG-Me), developed by Sugii *et al.*, is known to be able to separate HSA into its sub-types, which are classified based on the redox state of the thiol function of Cys^{34}.[9,10] The mechanism of separation is presumed to depend on conformational differences between HSA sub-types, which probably lead to a slight alteration in the electronic charge distribution on the surface of the molecule.[8,10] In the present study, HSA was separated into three main sub-types (HMA, HNA_{Cys}, and HNA_{oxy}) as has been reported in previous studies. When HSA was incubated with NAC, a new peak was formed, thus suggesting the formation of a new type of HSA having a conformation different from the intrinsic HSA sub-types. In the ^{14}C-labelled NAC assay, it was shown that this new type of HSA tightly retains NAC. This new type HSA can thus be attributed to an HSA-NAC conjugate *via* the thiol function of Cys^{34}. When comparing the present results with findings reported by Narazaki *et al.*, in which the covalent binding of other thiol-containing drugs (Captopril and Bucillamine derivatives) to HSA was investigated,[2,3] the newly formed HSA-drug conjugates, including HSA-NAC, appeared after the HNA_{oxy} peak. This finding is very interesting because the chemical structures of these thiol-containing drugs are quite different; the structure of NAC is similar to that of Cys. It is likely that HSA adopts a specific conformation when a thiol-containing drug binds to Cys^{34}, even if the structure of the drug differs.

The time-to-concentration profiles of the HSA sub-types show that HNA_{Cys} and HMA rapidly decreased and increased, respectively, immediately after the addition of NAC, while the HSA-NAC conjugate formed much more slowly. This observation suggests that NAC binds to HSA not directly but in a 2-step process. Specifically, in step-1, NAC rapidly attacks the disulfide bond of HNA_{Cys}, resulting in dissociation of Cys and an increase in HMA. NAC probably binds preferably to Cys and forms NAC-Cys mixed-disulfide at this time. In step-2, the low-molecular weight disulfides, such as NAC-Cys and probably NAC-NAC (diacetylcystine) as well as Cys-Cys (cystine), which were formed in the reaction mixture, slowly bind to the free-thiol of HMA and generate HSA_{NAC} or re-generate HNA_{Cys}.

In the present study, the binding kinetics of NAC was investigated using HSA purified from the renal failure patients as well as the healthy subjects in order to evaluate the pathological influence on the binding. Because Narazaki *et al.* has reported that the covalent protein-binding between HSA and Bucillamine was negatively well correlated to the HMA content of renal failure patient's serum, whereas such good correlations were not obtained in other pathological states.[6] Accordingly, we selected the renal failure as an appropriate pathological state for the binding analysis.

The rate constants difference between healthy and patient's HSA (**Table 1**) showed that the dissociation of Cys from HSA was suppressed in patients whereas the re-binding of Cys was not changed. This suggests that the high HNA_{Cys} and low HMA content of the patient's HSA is probably due to suppressed dissociation of Cys from HSA. On the other hand, the binding of NAC to HSA was facilitated in patient's HSA. Why these

changes occurred is not clear, but we have found that renal failure HSA resulted in a slight conformational change comparing with healthy HSA; (α-helical content: 63.3% for renal failure HSA, 67.8% for healthy HSA). Therefore, such conformational changes of renal failure patients' HSA may affect the binding and dissociation process of thiol-containing compounds through a structural change of the drug binding site, i.e. Cys^{34} moiety of albumin.

The present and previous[6] results suggest that an increase of covalent protein-binding formation in pathological state is common problem of thiol-containing drugs. Because such increase is thought to be mainly due to suppression of drug dissociation from albumin, the issues such as retardation of blood drug clearance, accumulation of drug in blood, and increase in blood level in repeated administration, should be considered in the therapy using thiol-containing drugs to patients. On the other hand, the free-thiol of Cys^{34} of albumin is thought to be physiologically important because it may acts as a radical scavenger[11,12] and a carrier of intrinsic various materials, such as metal ions.[1] Therefore, if thiol-containing drug highly occupies the free thiol of albumin in the pathological state, some unexpected adverse effect may occur.

With regard to drug-drug interactions, it is noteworthy that the dissociation of Cys from HSA induced by NAC occurs very rapidly. Because similar phenomena were observed in the reaction between HSA and both Captopril and Bucillamine derivatives,[2,3,6] it is believed that thiol-containing drugs can very rapidly dissociate Cys from HSA through a thiol-disulfide exchange reaction. Such reactions would be more rapid in the serum than in the buffer system because the thiol-disulfide exchange reaction is facilitated by factors such as dissolved oxygen and metal ions.[2] In fact, we have observed that the plasma free Cys level rapidly increased immediately after (2.5 min) an intravenous administration of pharmacological dose of NAC to rat.[13] This rapid "drive out" effect of thiol-drugs on Cys is estimated to applicable to the interaction between thiol-drugs, i.e., the already bound thiol-drug will be dissociated rapidly by combining with another thiol-containing compounds. Therefore, if a thiol-drug is used in combination with another thiol-drug in therapy, it should be considered that the free drug concentration of a thiol-drug may increase drastically after the administration of another thiol-drug.

In conclusion, we report that NAC interacts with HSA through a 2-step thiol-disulfide exchange reaction. NAC rapidly reduces the disulfide bond of HNA_{Cys} and dissociates Cys from HSA, and it then binds to HSA much more slowly. Kinetic analysis has clarified that the covalent binding of NAC to HSA involves mechanical properties that are shared with other thiol-containing drugs and that the binding kinetics may be affected by pathological state.

Acknowledgements: The authors thank Drs. Kenichiro Kitamura and Kimio Tomita (Department of Nephrology, Kumamoto University Graduate School of Medical Sciences, Kumamoto, Japan) for blood sample collection from hemodialysis patients and healthy subjects.

References

1) Carter, D. C. and Ho, J. X.: Structure of serum albumin. In Anfinsen, C. B., Edsall, J. T., Richards, F. M. and Eisenberg, D. S. (eds.): *Advances in Protein Chemistry*, Academic Press, San Diego, 1994, vol. **45**, pp. 153–203.

2) Narazaki, R., Harada, K., Sugii, A. and Otagiri, M.: Kinetic analysis of the covalent binding of Captopril to human serum albumin. *J. Pharm. Sci.*, **86**: 215–219 (1997).

3) Narazaki, R., Hamada, M., Harada, K. and Otagiri, M.: Covalent binding between Bucillamine derivatives and human serum albumin. *Pharm. Res.*, **13**: 1317–1321 (1996).

4) Harada, D., Naito, S., Hiraoka, I. and Otagiri, M.: *In vivo* kinetic analysis of covalent binding between N-acetyl-L-cysteine and plasma protein through the formation of mixed disulfide in rats. *Pharm. Res.*, **19**: 615–620 (2002).

5) Harada, D., Naito, S. and Otagiri, M.: Kinetic analysis of covalent binding between N-acetyl-L-cysteine and albumin through the formation of mixed disulfides in human and rat serum *in vitro*. *Pharm. Res.*, **19**: 1648–1654 (2002).

6) Narazaki, R. and Otagiri, M.: Covalent binding of a bucillamine derivative with albumin in sera from healthy subjects and patients with various diseases, *Pharm. Res.*, **14**: 351–353 (1997).

7) Watanabe, H., Tanase, S., Nakajou, K., Maruyama, T., Kragh-Hansen, U., and Otagiri, M.: Role of arg-410 and tyr-411 in human serum albumin for ligand binding and esterase-like activity. *Biochem. J.*, **349**: 813–819 (2000).

8) Sugii, A., Harada, K., Nishimura, K., Hanaoka, R. and Masuda, S.: High-performance liquid chromatography of proteins on N-methylpyridinium polymer columns. *J. Chromatogr.*, **472**: 357–364 (1989).

9) Nishimura, K., Harada, K., Masuda, S. and Sugii, A.: High-performance liquid chromatography of serum albumins on an N-methylpyridium polymer-based column. *J Chromatogr.*, **525**: 176–182 (1990).

10) Sugii, A.: Development of polymers for high performance ion-exchange chromatography and their application to analysis of human serum albumin components. *Yakugaku Zasshi*, **113**: 343–355 (1993).

11) Soriani, M., Pietraforte, D. and Minetti, M.: Antioxidant potential of anaerobic human plasma: role of serum albumin and thiols as scavengers of carbon radicals. *Arch. Biochem. Biophys.*, **312**: 180–188 (1994).

12) Pirisino, R., Di Simplicio, P., Ignesti, G., Bianchi, G.

and Barbera, P.: Sulfhydryl groups and peroxidase-like activity of albumin as scavenger of organic peroxides. *Pharmacol. Res. Commun.*, **20**: 545–552 (1988).
13) Harada, D., Naito, S., Kawauchi, Y., Ishikawa, K., Koshitani, O., Hiraoka, I. and Otagiri, M.: Determination of reduced, protein-unbound, and total concentrations of N-acetyl-L-cysteine and L-cysteine in rat plasma by post-column ligand substitution high-performance liquid chromatography. *Anal. Biochem.*, **290**: 251–259 (2001).

Available online at www.sciencedirect.com
SCIENCE DIRECT®
Biochimica et Biophysica Acta 1675 (2004) 21–31
BIOCHIMICA ET BIOPHYSICA ACTA
BBA
http://www.elsevier.com/locate/bba

Physicochemical characterization of cross-linked human serum albumin dimer and its synthetic heme hybrid as an oxygen carrier

Teruyuki Komatsu[a], Yukiko Oguro[a], Yuji Teramura[a], Shinji Takeoka[a], Junpei Okai[b], Makoto Anraku[b], Masaki Otagiri[b], Eishun Tsuchida[a,*]

[a]*Advanced Research Institute for Science and Engineering, Waseda University, 3-4-1 Okubo, Shinjuku-ku, Tokyo 169-8555, Japan*
[b]*Department of Pharmaceutics, Faculty of Pharmaceutical Sciences, Kumamoto University, 5-1 Oe-honmachi, Kumamoto 862-0973, Japan*

Received 13 May 2004; received in revised form 9 August 2004; accepted 10 August 2004
Available online 11 September 2004

Abstract

The recombinant human serum albumin (rHSA) dimer, which was cross-linked by a thiol group of Cys-34 with 1,6-bis(maleimido)hexane, has been physicochemically characterized. Reduction of the inert mixed-disulfide of Cys-34 beforehand improved the efficiency of the cross-linking reaction. The purified dimer showed a double mass and absorption coefficient, but unaltered molar ellipticity, isoelectric point (p*I*: 4.8) and denaturing temperature (65 °C). The concentration dependence of the colloid osmotic pressure (COP) demonstrated that the 8.5 g dL^{-1} dimer solution has the same COP with the physiological 5 g dL^{-1} rHSA. The antigenic epitopes of the albumin units are preserved after bridging the Cys-34, and the circulation lifetime of the ^{125}I-labeled variant in rat was 18 h. A total of 16 molecules of the tetrakis{(1-methylcyclohexanamido)phenyl}porphinatoiron(II) derivative (FecycP) is incorporated into the hydrophobic cavities of the HSA dimer, giving an albumin–heme hybrid in dimeric form. It can reversibly bind and release O_2 under physiological conditions (37 °C, pH 7.3) like hemoglobin or myoglobin. Magnetic circular dichroism (CD) revealed the formation of an O_2–adduct complex and laser flash photolysis experiments showed the three-component kinetics of the O_2-recombination reaction. The O_2-binding affinity and the O_2-association and -dissociation rate constants of this synthetic hemoprotein have also been evaluated.

Keywords: Human serum albumin dimer; Cross-linking; Colloid osmotic pressure; Synthetic heme; Albumin–heme dimer; Oxygen carrier

1. Introduction

Human serum albumin (HSA) is the most abundant plasma protein and contains 35 cysteines, of which 17 couples form intramolecular disulfide bonds to fold a single polypeptide as a unique heart-shape structure [1–4]. Only the first thiol residue in the chain, namely Cys-34, does not participate in the S–S bonding and functions as a binding site for the SH-involving ligands (cysteine, glutathione, and captopril), as well as for the various metal ions and nitric oxide [1,5]. Interestingly, two albumin molecules can associate to produce a dimer through an intermolecular disulfide bridge of Cys-34; approximately 5% of HSA is actually in a dimeric form in our bloodstream [6]. Hughes [7] initially prepared the HSA dimer by the addition of bifunctional $HgCl_2$, which causes Cys-34 to connect through mercury. Subsequent oxidation of this mercury dimer by treatment with iodine gave a disulfide-linked HSA [8]. It can also be directly prepared by oxidation of HSA with ferricyanide [9]. However, electron spin resonance measurements of HSA and the latest crystal structural analysis of the recombinant HSA (rHSA) revealed that Cys-34 locates in a hydrophobic crevice at a depth of 9.5 Å from the surface [2–4,10]. This implies that the intermolecular Cys-34 disulfide bridging might lead to flattening of the pocket. We have linked two rHSA molecules with a flexible bola-shape spacer, 1,6-bis(maleimido)hexane (BMH), which is long (16 Å) enough to connect the Cys-34 residues, to produce a new type of rHSA dimer (Fig. 1) [11].

* Corresponding author. Tel.: +81 3 5286 3120; fax: +81 3 3205 4740.
E-mail address: eishun@waseda.jp (E. Tsuchida).

0304-4165/$ - see front matter © 2004 Elsevier B.V. All rights reserved.
doi:10.1016/j.bbagen.2004.08.010

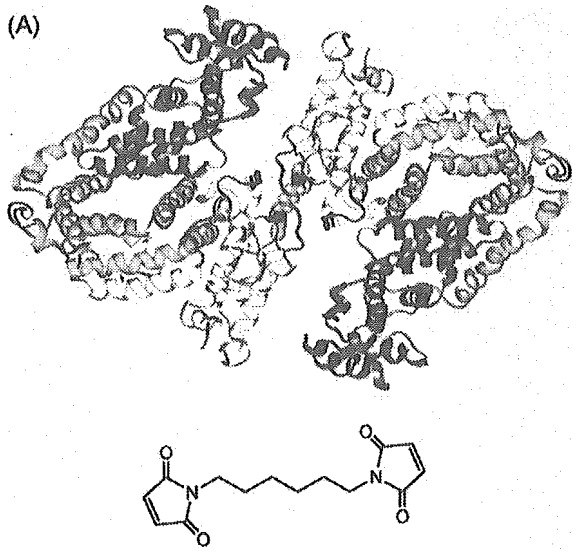

Fig. 1. (A) Simulated structure of rHSA dimer cross-linked by Cys-34 with 1,6-bis(maleimido)hexane (BMH). The domains I, II, and III of each rHSA unit are colored white, yellow, and pink, respectively. The cross-linking agent (BMH) is shown in a space-filling representation and colored by atom type (carbon: green, nitrogen: blue, oxygen: red). The figure was made with insight II (Molecular Simulations) on the basis of the 1e78 available at the Brookhaven PDB. (B) Formula of synthetic heme, FecycP.

On the other hand, a maximum of eight molecules of synthetic heme with a covalently bound proximal base is incorporated into the hydrophobic cavities of rHSA, giving an albumin–heme hybrid, which can reversibly bind and release O_2 under physiological conditions (pH 7.3, 37 °C) like hemoglobin (Hb) or myoglobin (Mb) [12]. We have shown that this O_2-carrying plasma protein acts as a red blood cell (RBC) substitute in vitro and in vivo [13]. The only fault of this system is its relatively low heme concentration, which reflects the O_2 solubility in the medium. For instance, the albumin–heme solution with a physiological HSA concentration (≈0.75 mM) involves 6 mM of heme, which corresponds to only 65% of the amount in human blood ([heme]=9.2 mM). A highly condensed solution can dissolve more heme, however, the colloid osmotic pressure (COP) increases in proportion to the albumin concentration. We have found that a total of 16 molecules of 2-[8-{*N*-(2-methylimidazolyl)}octanoyloxymethyl]-5,10,15,20-tetrakis{α,α,α,α-*o*-(pivalamido)phenyl}porphinatoiron(II) (FepivP) was incorporated into the BMH-bridged HSA dimer, and this solution with 0.75 mM HSA includes 12 mM of heme [11]. The tertiary structures of the two protein-units might be intact after the cross-linking, and the ligand-binding capacity of the dimer became twofold in excess relative to that of the monomer. Consequently, the saline solution of the albumin–heme dimer can transport a large volume of O_2 in comparison to the human blood while maintaining its COP on a physiological level. A long persistence in circulation due to the large molecular size is also expected. In this paper, we report the efficient synthesis, physicochemical characterization, and preliminary pharmacokinetics of the BMH-bridged rHSA dimer. Furthermore, the O_2-binding properties of the albumin-heme dimer incorporating the FepivP analogue, 2-[8-{*N*-(2-methylimidazolyl)}octanoyloxymethyl]-5,10,15,20-tetrakis{α,α,α,α-*o*-(1-methylcyclohexanamido)phenyl}porphinatoiron(II) (FecycP, Fig. 1), are evaluated by magnetic circular dichroism and laser flash photolysis.

2. Material and methods

2.1. Materials

An rHSA (Albrec®, 25 wt.%) was provided from the NIPRO (Osaka). Ethanol, dithiothreitol (DTT), 2,2′ -dithiopyridine, and warfarin (all high-purity grades) were purchased from Kanto Chemical, (Tokyo) and used without further purification. 1,6-Bis(maleimido)hexane was purchased from Pierce Biotechnology (Rockford, USA). Diazepam was purchased from Wako Pure Chemical Ind., (Tokyo). 2-[8-{*N*-(2-Methylimidazolyl)}octanoyloxymethyl]-5,10,15,20-tetrakis{α,α,α,α-*o*-(1-methylcyclohexanamido)phenyl}porphinatoiron(II) (FecycP) was prepared according to our previously reported procedure [14].

2.2. Synthesis of rHSA dimer

Aqueous DTT (1.0 M, 0.24 mL) was added to the phosphate buffer solution (pH 7.0, 10 mM) of rHSA (0.75 mM, 80 mL) under nitrogen, and the solution was quickly mixed by a vortex mixer, followed by an incubation for 30 min at room temperature. The obtained rHSA in reduced form was washed with a total of 880-mL phosphate buffer (pH 7.0, 2.25 mM) using an ADVANTEC UHP-76K ultrafiltration system with a Q0500 076E membrane (cutoff Mw 50 kDa) and finally condensed to 26.7 mL ([rHSA]=2.25 mM). The mercapto-ratio of the Cys-34

was confirmed by the reaction with 2,2′-ditiopyridine (2,2′-DTP), which immediately coupled with the free thiol group to give 2-thiopyridinone (2-TP) with an absorption at 343 nm [molar absorption coefficient (ε_{343}): 8.1×10^3 M^{-1} cm^{-1}]. Quantitative assay of the produced 2-TP showed that the mercapto-ratio of Cys-34 was 100%. Ethanolic BMH (6.38 mM, 4.76 mL) divided into three portions was then slowly added dropwise into the rHSA solution within 1 h under an N_2 atmosphere, and gently stirred overnight at room temperature. The reaction kinetics was observed by the HPLC measurements. The HPLC system consisted of a Shimadzu LC-8A pump and a Shimadzu SPD-10A UV detector. A Shodex Protein KW-803 column was used and the mobile phase was phosphate buffered saline (PBS, pH 7.4) at 25 °C (1.0 mL min^{-1}). The dimer was purified by gel column chromatography with Sephacryl S-200 HR (Pharmacia, 5 cmϕ×40 cm) and PBS (pH 7.4) as the eluant (5.0 mL min^{-1}). These separations were performed using a BIO-RAD EGP Combo Rec system. The elution was monitored by absorption at 280 nm. The purity of the dimer was measured by the HPLC technique described above. The albumin concentrations were assayed by general bromcresol green (BCG) methods using a Wako AlbuminB-Test [15].

2.3. Physicochemical properties

The UV–Vis absorption spectra were recorded on a JASCO V-570 spectrophotometer. The measurements were normally carried out at 25 °C. Circular dichroism (CD) spectra were obtained using a JASCO J-725 spectropolarimeter. The rHSA samples' concentration was 2 μM in PBS, and quartz cuvettes with a 1-mm thickness were used for the measurements over the range of 195–250 nm. The matrix associated laser desorption ionization time-of-flight mass spectra (MALDI-TOF MS) were obtained using a Shimadzu AXIMA-CFR Kompact MALDI, which was calibrated by BSA (Sigma A-0281) and HSA (Sigma A-3782). The specimens were prepared by mixing the aqueous sample solution (10 μM, 1 μL) and matrix (10 mg mL^{-1} sinapinic acid in 40% aqueous CH_3CN, 1 μL) on the measuring plate and drying in air. The viscosity and density of the rHSA solutions (PBS, pH 7.4) were obtained using an Anton PAAR DSC 300 capillary viscometer at 37 °C. The isoelectric points and molecular weights were obtained by a Pharmacia Phastsystem using isoelectric focusing (IEF) in Phast Gel IEF 3-9 and Native-PAGE in Phast Gel Gradient 8–25, respectively. The colloid osmotic pressures of the rHSA solutions (PBS, pH 7.4) were measured by a WESCOR 4420 Colloid Osmometer at 25 °C. A membrane filter with a 30-kDa cutoff was used. Differential scanning calorimetry (DSC) was measured on a SEIKO Instruments DCS120 differential scanning calorimeter at the scan rate of 1 °C min^{-1} in the temperature range between 10 and 95 °C. The concentrations of the rHSA samples were 75 μM in PBS (pH 7.4).

2.4. Ligand binding constants

The PBS solution of ligand (warfarin or diazepam, 20 μM, 2 mL) was mixed with the rHSA sample in PBS (20 μM, 2 mL), and the unbound ligand fractions were separated by centrifugation (2000 rpm, 25 °C, 20 min) using a Millipore Centriplus YM-50. Adsorption of the ligand molecules onto the filtration membranes was negligible. The unbound ligand concentrations were determined by UV–Vis spectroscopic measurements.

2.5. Compatibility with blood components in vitro

Fresh whole blood was obtained from Wistar rats (300 g, male, Saitama Experimental Animals Supply, Japan) and stored in heparinized glass tubes. The rHSA samples (PBS, pH 7.4) were then slowly added to the blood at 50 vol.% concentrations (whole volume 2 mL). After 30 min, 30 μL of the sample was mixed with 100 μL of a Terumo ACD-A solution, which was diluted in advance with pure water by 1:10 (v/v). The blood cell numbers of the obtained samples were counted using a Sysmex KX-21 blood cell counting device. Furthermore, one drop of the incubated sample of the blood with the rHSA dimer was microscopically observed using an Olympus IX50 microscope with an IX70 CCD camera.

2.6. Immunogenicity

The Tris–HCl buffer solutions (TBS, pH 7.4, 50 mM, 50 μL) of the rHSA samples (10 μg mL^{-1}) were injected into a Nunc immunoplate and incubated at 4 °C overnight. The rHSA solutions in the wells were washed with TBS, and 2% skimmed milk was added to avoid the nonspecific binding of the antibody. After washing with TBS including 0.1% Tween 20 (Tween 20–TBS), anti-HSA polyclonal antibody (50 μL per well) was added and incubated for 2 h at 25 °C. The antibody was removed by aspiration, and 50 μL of horseradish peroxidase-labelled rabbit anti-IgG polyclonal antibody diluted 1/5000 by Tween 20–TBS was injected, following an incubation for 1 h at 25 °C. Finally, 100 μL of *o*-phenylenediamine substrate solution (400 mg mL^{-1} in 0.15 M citrate-phosphate buffer (pH 5.0) involving 0.1% H_2O_2) was put into each well. H_2SO_4 (2 M; 50 μL) was then added to stop the reaction. The resulting absorbance in each well was measured at 490 nm using a Japan InterMed Imunomini NJ-2300.

2.7. Circulation lifetime in vivo

The 125-Iodinated rHSA monomer and dimer were prepared by our previously reported procedures, and purified using a Pharmacia Bio-Gel PD-10 column [16]. The recovered ^{125}I-albumin had a specific activity of 2.0×10^7 cpm μg^{-1}, and was diluted by non-labeled albumin before intracardial administration into anesthetized Wistar rats

(200–210 g, male). The kinetics of the albumin clearance from the circulation was monitored by measuring the radioactivity in the plasma phase of blood taken from the lateral tail veins using an Aloka ARC 2000 Autowell Gamma Counter. Acid precipitability of the recovered radioactivity was also measured. The aqueous trichloroacetic acid (TCA, 25%, 0.1 mL) was first added to the plasma (20 μL) diluted with 5 g dL^{-1} rHSA (80 μL), followed by centrifugation (3000 rpm, 10 min). The precipitate was then washed with 12.5% TCA (0.2 mL) and the radioactivity of the pellet was measured. The rats were sacrificed at the end of the experiments by hemorrhage. The radioactivity of the excised organs was also measured as well. The care and handling of the animals were in accordance with NIH guidelines.

2.8. Preparation of albumin–heme dimer

The preparation of rHSA–FecycP dimer was carried out by mixing the EtOH solution of carbonyl-FecycP and an aqueous phosphate buffer solution of rHSA according to our previously reported procedures ([FecycP]/[rHSA]=16:1 (mol/mol)) [13]. The albumin concentrations were assayed by the general BCG methods described above, and the amount of FecycP was determined by the assay of the iron ion concentration using inductively coupled plasma spectrometry (ICP) with a Seiko Instruments SPS 7000A spectrometer.

2.9. Magnetic circular dichroism (MCD)

MCD spectra for the phosphate buffer solution of the rHSA–FecycP dimer (10 μM) under N_2, CO, and O_2 atmospheres were measured using a JASCO J-820 circular dichrometer fitted with a 1.5-T electromagnet. The accumulation times were normally three, and from each data point was subtracted the spectra without an electromagnetic (at 0 T) as the baseline.

2.10. O_2-Binding equilibrium and kinetics

O_2-Binding to FecycP was expressed by Eq. (1).

$$\mathrm{FecycP} + \mathrm{O_2} \underset{k_{off}}{\overset{k_{on}}{\rightleftharpoons}} \mathrm{FecycP(O_2)} \quad (K = k_{on}/k_{off}) \tag{1}$$

The O_2-binding affinity (gaseous pressure at half O_2-binding for heme, $P_{1/2}=1/K$) was determined by spectral changes at various partial pressure of O_2 as in previous reports [12,a,d,i4]. The FecycP concentrations of 20 μM were normally used for the UV–Vis absorption spectroscopy. The spectra were recorded within the range of 350–700 nm. The half lifetime of the dioxygenated species of the rHSA–FecycP dimer was determined by the time dependence of the absorption intensity at 549 nm, which is based on the O_2–adduct complex. The association and dissociation rate constants for O_2 (k_{on}, k_{off}) were measured by a competitive rebinding technique using a Unisoku TSP-600 laser flash photolysis apparatus [12,17–19]. The absorption decays accompanying the O_2 association to the rHSA–FecycP dimer obeyed three-component kinetics. We employed triple-exponentials to analyze the absorption decays; $\Delta A(t)$ [12,a,b,],

$$\Delta A(t) = C_1\exp(-k_1 t) + C_2\exp(-k_2 t) + C_3\exp(-k_3 t) \tag{2}$$

where k_1, k_2, k_3 are apparent rate constants for the each reaction. The data were fit to this equation using a Solver in Excel 2003.

3. Results and discussion

3.1. Synthesis of rHSA dimer

In the neutral pH range (5.0–7.0), DTT selectively reduces the mixed-disulfide of Cys-34 in HSA or BSA [20–22]. In fact, the addition of the small molar excess DTT into the rHSA solution (phosphate buffer, pH 7.0, 10 mM) under an N_2 atmosphere led to complete reduction of Cys-34 (mercapto-ratio became 100%). After removing DTT, ethanolic BMH was dropwise added to the reduced rHSA to initiate the cross-linking reaction. The pretreatment with DTT significantly increased the yield of the dimer, and the rHSA concentration of 15 g dL^{-1} gave the highest yield of 45%, which is significantly improved from our previous result (Fig. 2) [11]. Several attempts to facilitate the dimerization

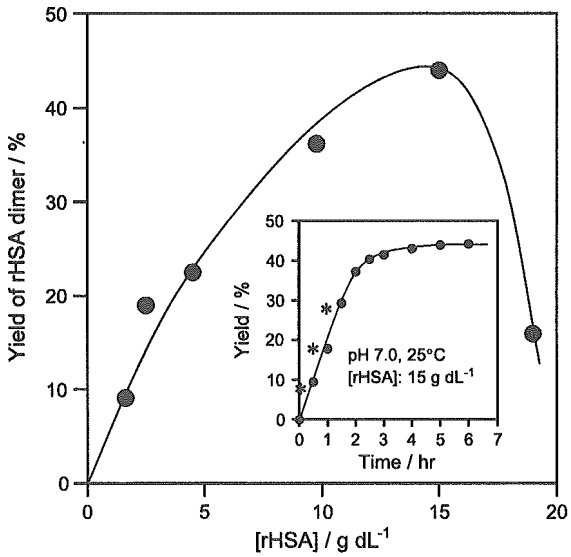

Fig. 2. The relationship between the rHSA concentration and yield of the rHSA dimer. The yields were determined based on the peak area in the HPLC elution curves. Inset shows the time course of the dimerization yield when the rHSA concentration was set at 15 g dL^{-1}. The asterisks indicate the time points when the EtOH solution of BMH was dropwise added. The total EtOH content in the reaction mixture was 15 vol.%.

unfortunately failed: (i) gentle heating (25–50 °C), (ii) changing the co-solvent from EtOH to DMF for dissolving the BMH, and molar ratio [BMH]/[rHSA]: 0.5–1.5, (iii) increasing the concentrations of co-solvents (<30%), and (iv) the further addition of the reactive rHSA monomer.

The HPLC elution curve of the reactant demonstrated only two peaks (rHSA monomer and dimer), which means that the bifunctional BMH was successfully bound to Cys-34 which led to dimer formation and not polymerization (Fig. 3). The yield reached a peak within 4 h (Fig. 2 inset). The addition of EtOH to the mixture (40 vol.%) immediately formed a white precipitate; this is similar to the well-known Cohn's methods [1,23]. However, the precipitate still contained the monomer component. In contrast, separation using gel column chromatography with Sephacryl S-200 HR gave the dimer with 99% purity and 80% recovery. Native-PAGE showed a single band in the molecular weight range of 13 kDa (Fig. 3, above). We could not detect the free thiol in the isolated rHSA dimer (mercapto-ratio: 0%), which is now available in gram quantities. The appearance of the obtained dimer solution (in PBS, 20 g dL^{-1}) did not change over 1 year at room temperature and underwent no aggregation and precipitation.

3.2. Physicochemical properties

The matrix associated laser desorption ionization time-of-flight mass spectroscopy (MALDI-TOF MS) of the BMH-bridged rHSA dimer showed a distinct sharp signal at *m/z* 132,741.3, which is in good agreement with the calculated mass (Mw. 133,179.6); the difference was only 0.3% (Table 1). The magnitudes of its UV–Vis absorption (λ_{max}: 280 nm) significantly increased compared to that of

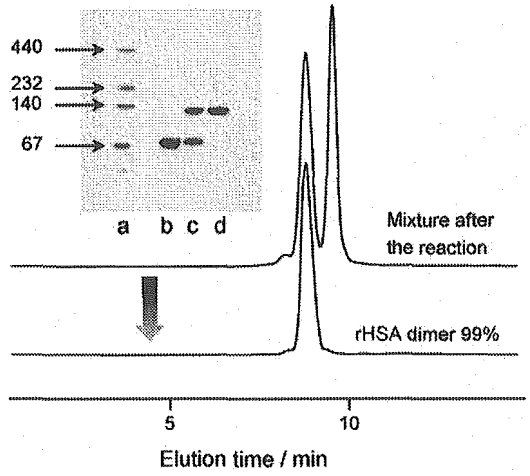

Fig. 3. HPLC elution curves of the rHSA dimer at 25 °C. The upper profile after the reaction indicated that the reactant consists of only the monomer and dimer. After gel column chromatography, the rHSA dimer was isolated with the purity of 99%. The left upper pattern is the native-PAGE electrophoresis of the rHSA dimer. a: markers, b: rHSA, c: mixture after the reaction, d: purified rHSA dimer.

Table 1
Physicochemical properties of rHSA dimer

	rHSA	rHSA dimer
Mw (Da)	66,331[a]	132,741[a]
	66×10^3 [b]	136×10^3 [b]
[calculated value]	66,451	133,180
Cys-34 mercapto ratio (%)	17	0
p*I*	4.8	4.8
ε_{280} (cm^{-1} M^{-1})	3.4×10^4	6.8×10^4
$[\theta]_{208}$ (deg cm^2 $dmol^{-1}$)	1.9×10^4	1.9×10^4
$[\theta]_{222}$ (deg cm^2 $dmol^{-1}$)	1.8×10^4	1.8×10^4

[a] Determined by MALDI-TOF/MS.
[b] Determined by [C] vs. COP/[C] (Fig. 5, inset).

rHSA with the same molar concentrations (Fig. 4(A)). The concentration of the albumin was carefully assayed by (i) BCG method [15] and (ii) weighing method with the weight of the freeze-dried sample and its molecular weight. While the molar absorption coefficient at 280 nm (ε_{280}: 6.8×10^4 M^{-1} cm^{-1}) became exactly twice the monomer's value (3.4×10^4 M^{-1} cm^{-1}), the CD spectral pattern (λ_{min}: 208, 222 nm) and the molar ellipticities at 208 and 222 nm ($[\theta]_{208}$: 1.9×10^4 deg cm^2 $dmol^{-1}$, $[\theta]_{222}$: 1.8×10^4 deg cm^2 $dmol^{-1}$) were identical to those of the monomer (Fig. 4(B), Table 1) [24,25]. It is appropriate to consider that the α-helix content of the each rHSA unit (67%) was unaltered [1–4]. The isoelectric point of the dimer (*p*I: 4.8) was also the same as that of rHSA. All these observations suggested that the secondary/tertiary structure and surface net charges of the rHSA units in the dimer did not change after the S–S disulfide bridging of Cys-34.

The DSC thermogram of this rHSA dimer showed an exothermic peak at 65 °C, which corresponds to its denaturing temperature (T_d). It has been shown that the T_d of HSA is largely dependent on the content of the

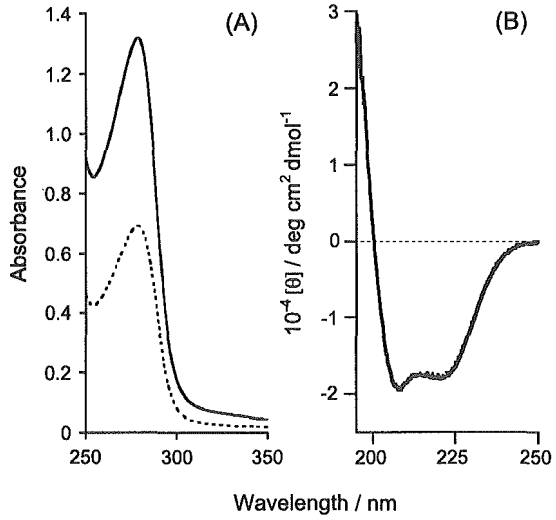

Fig. 4. (A) UV–Vis absorption spectra and (B) CD spectra of rHSA monomer (dotted line) and rHSA dimer (solid line) in PBS solution (pH 7.4) at 25 °C.

incorporated fatty acid, pH, and ionic strength [26,27]. In general, pasteurization for plasma HSA is performed at 60 °C for 10 h to eliminate the contaminations, e.g., hepatitis, HIV, and herpes virus [1]. Sodium caprylate and sodium *N*-acetyl-L-tryptophanate are commonly added to stabilize the albumin structure during the heat treatment [26]. Since the thermogram of the rHSA monomer under our sample conditions (PBS, pH 7.4) showed the T_d at 63 °C, we concluded that the rHSA dimer has the same thermodynamic stability with the monomer. Only the enthalpy change during the denaturation (ΔH) was slightly lower than the twice the monomer's value.

HSA acts as a carrier for many endogenous and exogenous substances in the blood circulation, and has two major specific drug binding sites, namely the warfarin site (Site I) and the indole and benzodiazepine site (Site II) [1,28]. We then determined the binding constants of typical ligands, warfarin (Site I-ligand) and diazepam (Site II-ligand), for the rHSA dimer using the ultracentrifugation method. In contrast to the results of the control experiments with rHSA, the amount of unbound ligand decreased to nearly half. The equilibria are expressed by following equations:

$$D + L \underset{}{\overset{K_1}{\rightleftharpoons}} D\text{-}L \quad (3)$$

$$D\text{-}L + L \underset{}{\overset{K_2}{\rightleftharpoons}} D\text{-}L_2 \quad (4)$$

$$D + 2L \underset{}{\overset{K_1K_2}{\rightleftharpoons}} D\text{-}L_2 \quad (5)$$

where D is the rHSA dimer and L represents the ligand. The apparent binding constants (K_1K_2) of the warfarin and diazepam to the dimer were calculated to be 9.2×10^{10} and 3.0×10^{10} M^{-2}, respectively. If the each albumin unit independently accommodates one ligand, we estimated K_1 ($=K_2$) of each ligand as the square root of these values; 3.0×10^5 and 1.7×10^5 M^{-1}, respectively. They are almost in the same range as the binding constants for the monomeric rHSA (K_1), 3.8×10^5 and 1.4×10^5 M^{-1}, which means that neither the prevention nor the cooperation of the second ligand binding occurred in the dimer.

The attempt to prepare single crystals of the rHSA dimer for X-ray structural analysis failed, probably because it is likely to be very flexible at the BMH moiety. Transmission electron microscopy of the negatively stained samples showed homogeneous round particles with a diameter of 15–20 nm (not shown), however, the image is too small to obtain precise morphological information about the molecule.

The primary physiological function of HSA is the maintenance of COP within the blood vessels. Although HSA accounts for only 60% of the mass of the plasma protein, it contributes 80% of the COP. Two-thirds of this COP is simply the van't Hoff pressure and the other third arises from the Donnan effect of the negative charges of the plasma proteins, which is essentially due to albumin [1]. The relationship between the protein concentration and COP was observed for the rHSA and rHSA dimer solutions (Fig. 5). Both lines deviated upward from the linear correlation, because of the relatively larger value of the second virial coefficient, which is an index of the COP capacity, of the albumin molecule compared to those of the other plasma proteins. The measured rHSA monomer's curve coincided well to the previously reported result of Scatchard and co-workers (dotted line) [29]. The physiological concentration (5 g dL^{-1}) of rHSA represented the COP of 19 Torr. The careful inspections of their COP curves revealed that the 8.5 g dL^{-1} dimer solution has the same COP as the 5 g dL^{-1} rHSA. The plots of [C] versus COP/[C] gave a straight line, and the extrapolations to the y intercept afford the molecular weights of the monomer and dimer of 66×10^3 and 136×10^3 Da, respectively.

3.3. Viscosity and compatibility with blood components

Viscosity is a characteristic of proteins related to their size, shape, and conformation. The PBS solution of 8.5 g dL^{-1} rHSA dimer exhibited a Newtonian flow similar to the 5.0 g dL^{-1} rHSA, and showed a viscosity of 1.2 cP at a shear rate of 230 s^{-1} (Fig. 6). The dimer solution was then mixed with freshly drawn whole blood (1:1, v/v). The obtained suspension did not show any coagulation or precipitation for 6 h at 37 °C (after 6 h, hemolysis gradually took place even in the control experiment with saline or rHSA), and its viscosity profile was again Newtonian (1.8 cP at 230 s^{-1}). This result demonstrated good compatibility of the rHSA dimer with blood.

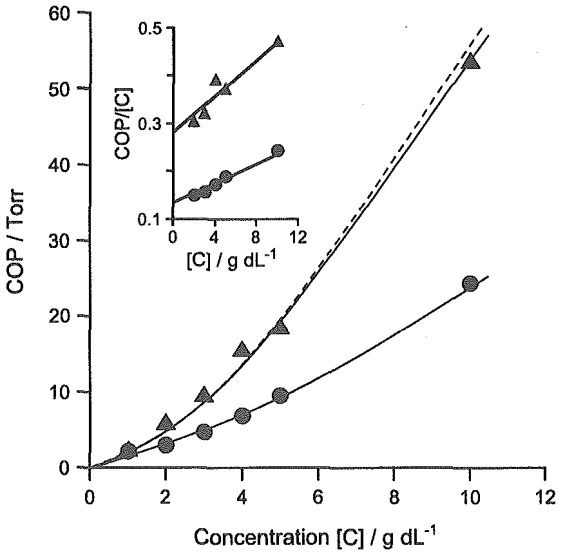

Fig. 5. Concentration [C] dependence of COP of rHSA monomer (▲) and rHSA dimer (●) in PBS (pH 7.4) at 22 °C. The dotted line represents the plasma HSA results taken from Ref. [29]. Inset shows relationship between [C] and COP/[C] for rHSA monomer (▲) and rHSA dimer (●).

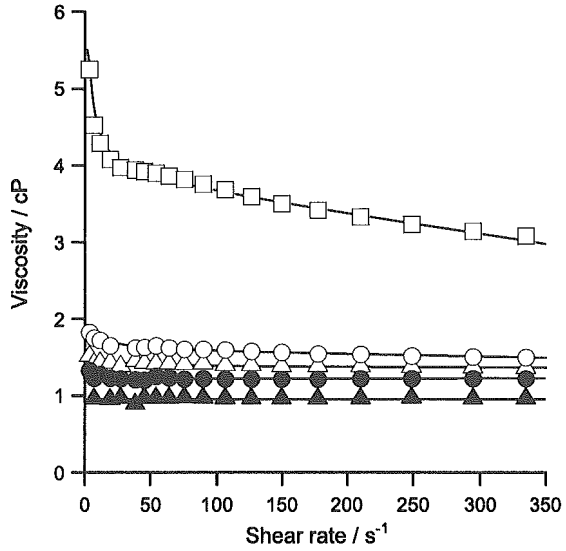

Fig. 6. Changes in the viscosity of rHSA monomer and rHSA dimer at various shear rates at 37 °C [□: whole blood, ●: 8.5 g dL^{-1} rHSA dimer, ▲: 5.0 g dL^{-1} rHSA, ○: 8.5 g dL^{-1} rHSA dimer plus whole blood (1:1, v/v), △: 5.0 g dL^{-1} rHSA plus whole blood (1:1, v/v)].

In order to evaluate the blood compatibility of the 8.5 g dL^{-1} rHSA dimer solution in detail, the changes in the number of blood cell components [RBC, white blood cells (WBC), and platelets (PLT)] have been counted after the mixture (1:1, v/v). The numbers just after the addition of the rHSA dimer to the whole blood were reasonably reduced to half the basal values; the same behavior was observed in the control experiments with the saline or 5 g dL^{-1} rHSA [Fig. 7(A)]. Optical microscopic observations revealed that the homogeneous round shape of the RBCs was completely retained [Fig. 7(B)(C)]. Therefore, it can be considered that no specific interaction occurred between the rHSA dimer and the blood cell components in vitro.

3.4. Immunogenicity

We then analyzed the immunological reactivity of the rHSA dimer against the anti-HSA polyclonal antibody. The absorption intensity of the reactant plate with the dimer showed clear concentration dependence in the same manner as those of the rHSA and plasma HSA groups (Fig. 8). It is known that HSA has five major antigenic sites by analysis using synthetic peptides [30,31]. The sites are nearly α-helical regions in the HSA molecule and include charged and/or aromatic residues which are important for the presentation of antigenic determinations. We previously reported that the cross-reactivity of the anti-HSA polyclonal antibody to BSA was extremely low, despite their homologies of the sequences over 70% and its antigenic sites in the same regions [32]. The antigenic epitopes of rHSA are preserved after bridging the Cys-34.

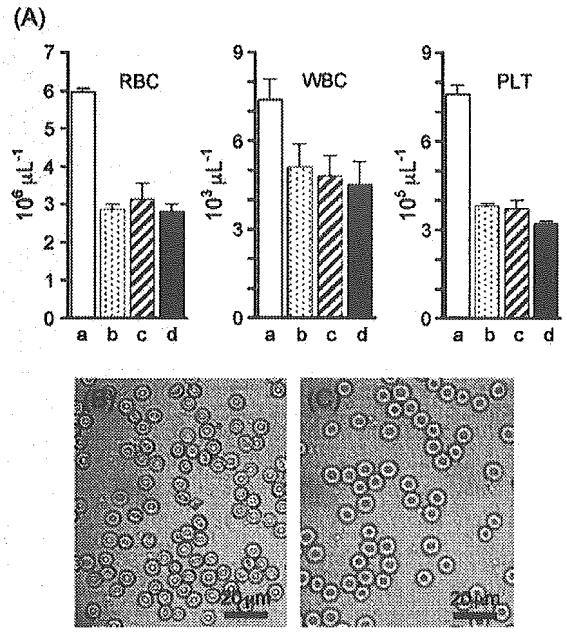

Fig. 7. (A) The blood cell (RBC, WRC, PLT) numbers in the blood suspension with the rHSA samples (1:1, v/v) at 25 °C [a: whole blood (basal value), b: with saline, c: with 5.0 g dL^{-1} rHSA, d: with 8.5 g dL^{-1} rHSA dimer]. Optical microscopic observations of (B) whole blood and (C) the blood suspension with the 8.5 g dL^{-1} rHSA dimer (1:1, v/v) (bar: 20 μm). The shape of the RBC with a diameter of ca. 8 μm did not change.

3.5. Circulation lifetime of ^{125}I-labeled rHSA dimer in rats

The rHSA and rHSA dimer labeled with ^{125}I were injected into rats to determine their blood circulation

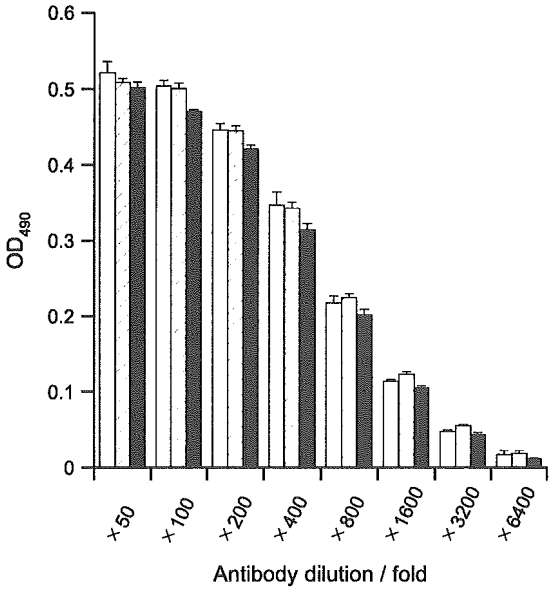

Fig. 8. Cross-reactivity of the anti-HSA polyclonal antibody with rHSA monomer and rHSA dimer [white bar: plasma HSA, diagonal bar: rHSA monomer, black bar: rHSA dimer]. All values are mean±S.D. (n=3).

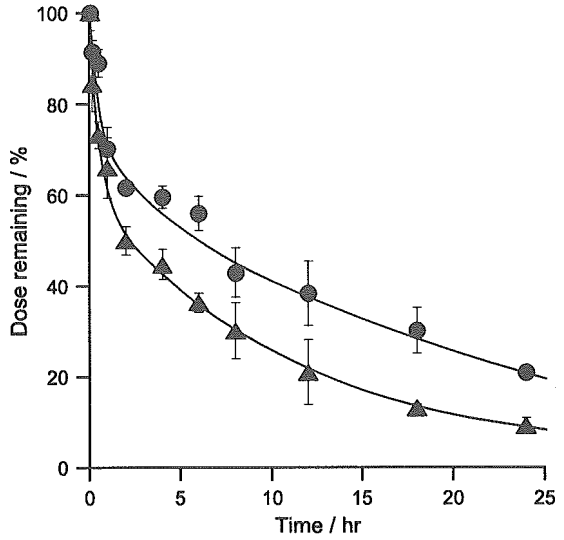

Fig. 9. Plasma levels of ^{125}I-rHSA monomer and dimer (1.0×10^7 cpm, 1.0 mg kg^{-1}) after intracardial administration into Wistar rats. All values are mean±S.D. (n=3).

lifetimes. The time courses of the radioactivity clearly showed two-phase kinetics, and significant differences between these two samples (Fig. 9). The half lifetimes ($\tau_{1/2}$) determined from the disappearance phase (β-phase) were 8.9 and 16.2 h for the monomer and dimer, respectively. The enlargement of the molecular size definitely led to retardation of extravasation through the vascular endothelium and produced a longer lifetime in the bloodstream. Radioactivity of the trichloroacetic acid precipitates recovered up to 95% the intensity, which means ^{125}I did not dissociate from the proteins. The tissue distributions of the rHSA dimer were in the skin, liver, kidney, and spleen (not shown), which took up most of the radioactivity, and we could not find any differences to that of the rHSA monomer.

More recently, McCurdy et al. [33] reported that a reiterated form of recombinant rabbit serum albumin (rRSA), in which two copies of the C34A rRSA mutant were joined with the C-terminus and N-terminus by a hexaglycine spacer, was more rapidly cleared ($\tau_{1/2}$: 3.0 days) in vivo (rabbit) than the corresponding monomer, C34A rRSA ($\tau_{1/2}$: 4.9 days). They postulated that the mechanism of this quick clearance of the dimer appears to involve the reticuloendothelial system (two binding sites on a dimer molecule to phagocytic cells may underlie the increased rate); and also suggested that the albumin dimerization through Cys-34 probably does not substantially contribute to the albumin metabolism. However, our results clearly showed that the Cys-34 BMH-bridged rHSA dimer has the longer circulation lifetime relative to that of the rHSA monomer. This opposite conclusion presumably arises from the differences in the chemical structure of the cross-linking agents, highly-ordered structure of the albumin dimer itself, and mammal species in the experimental protocol.

3.6. Albumin–heme dimer and its O_2-binding

Since a maximum of eight FecycPs (Fig. 1) was incorporated into certain domains of rHSA [12,d,], we postulated that the rHSA dimer can capture a twofold molar excess of FecycP molecules relative to the monomer. From the quantitative analyses of the amount of rHSA and FecycP in the hemoprotein, the ratio of the FecycP/rHSA (mol/mol) was determined to be 15.7 for the mixing ratio (m) of 16 and 16.4 for the m of 20. Thus, we concluded that the maximum binding numbers of FecycP to an rHSA dimer were 16, the same as FepivP [11]. The obtained red-solution of the rHSA–FecycP dimer was stored for more than 1 year at 4 °C without any aggregation and precipitation.

The UV–Vis absorption spectrum of the aqueous rHSA–FecycP dimer solution in an N_2 atmosphere showed the formation of a typical five-N-coordinate high-spin complex of porphyrinatoiron(II) (λ_{max}: 444, 539, 565 nm) [12,14,17,19]. Upon exposure of this solution to O_2, the absorption spectral pattern immediately changed to that of a dioxygenated species (λ_{max}: 426, 549 nm). This O_2-binding reaction was reversible and kinetically stable under physiological conditions (pH 7.3, 37 °C). After admitting the CO gas, the O_2–addcut complex moved to the very stable carbonyl low-spin complex (λ_{max}: 427, 539 nm) (Fig. 10).

We then employed MCD spectroscopy to characterize the coordination structure of the FecycP in the rHSA dimer. Under an N_2 atmosphere, the MCD showed a well-characterized spectrum of a mono-imidazole ligated five-

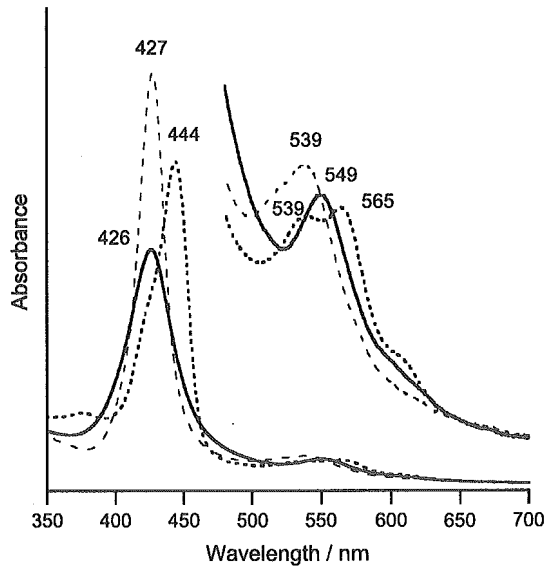

Fig. 10. UV–Vis absorption spectral changes of the rHSA–FecycP dimer in phosphate buffer solution (pH 7.3) at various conditions (25 °C) (dotted line: under N_2; solid line: under O_2; broken line: under CO).

coordinate high-spin porphyrinatoiron(II), which is in contrast to that of the six-coordinate low-spin state with the bis-imidazole ligated complex (Fig. 11) [34]. This observation indicates that no amino acid residue binds to the sixth position of FecycP in the rHSA structure under an N_2 atmosphere. The admission of O_2 gas yields an S-shaped A-term MCD in the Soret-band region, which shows the formation of an O_2–adduct complex as observed in the spectra of the other dioxygenated porphyrinatoiron(II) [34]. The CO adduct is also low spin and showed a similar A-term MCD band with a strong intensity. In all cases, the pattern in the Q-band regions coincided well with those reported previously [34].

The autooxidation reaction of the oxy state (λ_{max}: 549 nm) slowly occurred and the absorption intensity of 549 nm almost disappeared after 36 h, leading to the formation of the inactive Fe(III)cycP. The half-life of the dioxygenated species ($\tau_{1/2}$) was 6 h at 37 °C, which is significantly longer than that of our previous results for the rHSA–FepivP dimer ($\tau_{1/2}$: 2 h) [11]. The hydrophobic cyclohexanoyl fences on the porphyrin ring plane could effectively retard the autooxidation through the proton-driven process.

3.7. O_2-Binding kinetics and equilibrium of albumin–heme dimer

The association and dissociation rate constants for O_2 (k_{on}, k_{off}) were explored by laser flash photolysis. The absorption decays accompanying the O_2 recombination were composed of three-component kinetics, and the curves were fit by a triple-exponential equation [12,a,b,14]. The minor (less than 12%) component k_1, which is the fastest rate constant, is presumably correlated with a base elimination reaction [35]. From the slope of the linear plots of k_2 and k_3 versus the O_2 concentration, two association rate constants for the fast O_2 rebinding (k_{on}) and the slow O_2 rebinding were obtained (Table 2). The k_{on} values are 5.8-fold grater than k'_{on}, and the amplitude ratio of the fast and slow reactions was approximately 5/3. The O_2 association to FecycPs incorporated in the certain domains of the rHSA dimer is largely influenced by the protein environments surrounding each iron center of FecycP, for example, steric hindrance by the amino acid residues and/or difference in polarity. Six of the 16 sites of FecycP in the rHSA dimer are estimated to be the slow sites for the O_2 association.

Table 2
O_2-Binding parameters of the rHSA–FecycP dimer in phosphate buffer solution (pH 7.3) at 25 °C

	k_{on} (M^{-1} s^{-1})	k'_{on} (M^{-1} s^{-1})	k_{off} (s^{-1})	k'_{off} (s^{-1})	$P_{1/2}$ (Torr)[a]
rHSA–FecycP dimer	2.8×10^7	4.8×10^6	6.7×10^2	1.2×10^2	38
rHSA–FecycP	4.6×10^7	7.3×10^6	9.8×10^2	1.6×10^2	35
Hb (T-state)[b]	2.9×10^6		1.8×10^2		40

[a] At 37 °C. [b]pH 7.0, 20 °C, from Ref. [36].

The O_2-binding affinity ($P_{1/2}$) of the rHSA–FecycP dimer was determined to be 38 Torr at 37 °C on the basis of the UV–Vis spectral changes by O_2 titration [12,14,17–19]. The obtained $P_{1/2}$ is very close to that of rHSA–FecycP in the monomeric form and T-state Hb (Table 2) [12,d,35]. The O_2-dissociation rate constants were also calculated by k_{on}/K.

The rHSA–FecycP dimer did not show a cooperative O_2-binding profile like that seen in RBC; the Hill coefficient was 1.0 (Fig. 12). Although $P_{1/2}$ is slightly lower than that of RBC, the O_2-transporting efficiency (OTE) of the rHSA–FecycP dimer between the lungs (P_{O_2}: 110 Torr) and muscle

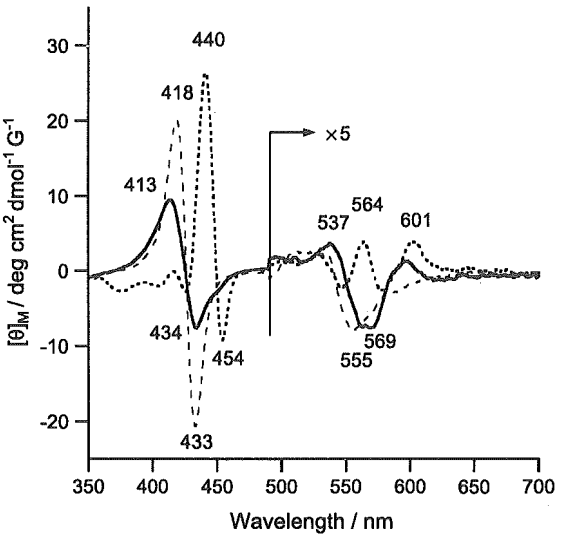

Fig. 11. MCD spectral changes of the rHSA–FecycP dimer in phosphate buffer solution (pH 7.3) at various conditions (25 °C) (dotted line: under N_2; solid line: under O_2; broken line: under CO).

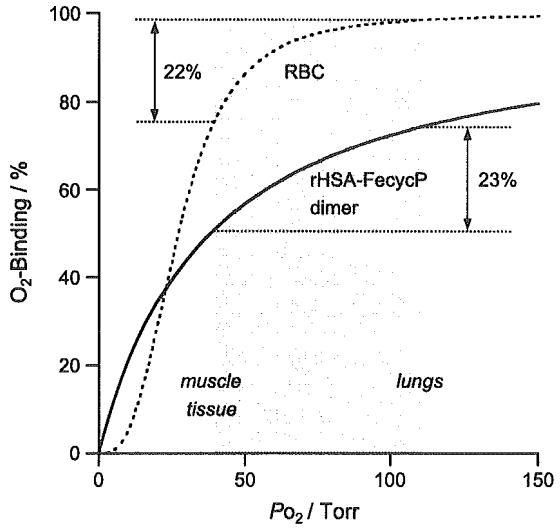

Fig. 12. OEC curve of the rHSA–FecycP dimer at 37 °C.

tissue (P_{O_2}: 40 Torr) (23%) becomes slightly higher than that of the human RBC (22%).

4. Conclusions

The obvious characteristics of the rHSA dimer cross-linked with the bola-shaped bismaleimide are as follows: (i) unaltered essential properties of the albumin units (the secondary/tertiary structure, surface net charges, thermostability), (ii) excess ligand-binding capacity relative to the monomer while maintaining its COP at the physiological value, (iii) good blood compatibility and identical antigenic epitopes with the monomer, and (iv) longer half-life in the bloodstream and similar tissue distributions with rHSA. Furthermore, (v) one molecule of the rHSA dimer incorporates 16 FecycPs, which is exactly twice the amount compared to that of the monomeric rHSA, and the obtained hemoprotein can reversibly bind and release O_2 under physiological conditions. (vi) The 8.5 g dL^{-1} rHSA–FecycP dimer solution satisfies the initial clinical requirements for the O_2-carrier as an RBC substitute, which transports 10 mM O_2 (compared to 9.2 mM in the human blood) while maintaining the COP at a constant 19 Torr.

Acknowledgements

This work was partially supported by Grant-in-Aid for Scientific Research (no. 16350093) from JSPS, and Grant-in-Aid for Exploratory Research (no. 16655049) from MEXT Japan, and Health Science Research Grants (Regulatory Science) from MHLW Japan.

References

[1] T. Peters Jr., All about Albumin. Biochemistry, Genetics, and Medical Applications, Academic Press, San Diego, 1996, and reference therein.
[2] D.C. Carter, J.X. Ho, Structure of serum albumin, Adv. Protein Chem. 45 (1994) 153–203.
[3] S. Curry, P. Brick, N.P. Franks, Fatty acid binding to human serum albumin: new insights from crystallographic studies, Biochim. Biophys. Acta 1441 (1999) 131–140.
[4] S. Sugio, A. Kashima, S. Mochizuki, M. Noda, K. Kobayashi, Crystal structure of human serum albumin at 2.5 Å resolution, Protein Eng. 12 (1999) 439–446.
[5] DJ. Meyer, H. Kramer, N. Özer, B. Coles, B. Ketterer, Kinetics and equiliburia of *S*-nitrosothiol–thiol exchange between glutathione, cysteine, penicillamines and serum-albumin, FEBS Lett. 345 (1994) 177–180.
[6] T. Peters Jr., Serum albumin, Adv. Protein Chem. 37 (1985) 161–245.
[7] a W.L. Hughes, The proteins of blood plasma, in: H. Neurath, K. Bailey (Eds.), The Proteins, vol. IIB, Academic Press, New York, 1954, pp. 663–734;
b W.L. Hughes, H.M. Dintzis, Crystallization of the mercury dimers of human and bovine mercaptalbumin, J. Biol. Chem. 239 (1964) 845–849.
[8] R. Straessle, A disulfide dimer of human mercaptalbumin, J. Am. Chem. Soc. 76 (1954) 3138–3142.
[9] L.-O. Anderson, Hydrolysis of disulfide bonds in weakly alkaline media II. Bovine serum albumin dimer, Biochim. Biophys. Acta 117 (1966) 115–133.
[10] C.N. Cornell, R. Chang, L.J. Kaplan, The environment of the sulfhydryl group in human plasma albumin as determined by spin labeling, Arch. Biochem. Biophys. 209 (1981) 1–6.
[11] T. Komatsu, K. Hamamatsu, E. Tsuchida, Cross-linked human serum albumin dimer incorporating sixteen (tetraphenylporphinato)iron(II) derivatives: synthesis, characterization, and O_2-binding property, Macromolecules 32 (1999) 8388–8391.
[12] (a) E. Tsuchida, T. Komatsu, Y. Matsukawa, K. Hamamatsu, J. Wu, Human serum albumin incorporating tetrakis(*o*-pivalamido)phenylporphinatoiron(II) derivative as a totally synthetic O_2-carrying hemoprotein, Bioconj. Chem. 10 (1999) 797–802;
(b) T. Komatsu, Y. Matsukawa, E. Tsuchida, Kinetics of CO and O_2 binding to human serum albumin–heme hybrid, Bioconj. Chem. 11 (2000) 772–776;
(c) T. Komatsu, Y. Matsukawa, E. Tsuchida, Reaction of nitric oxide with synthetic hemoprotein, human serum albumin incorporating tetraphenylporphinatoiron(II) derivatives, Bioconj. Chem. 12 (2001) 71–75;
(d) T. Komatsu, Y. Matsukawa, E. Tsuchida, Effect of heme structure on O_2-binding properties of human serum albumin–heme hybrids: intramolecular histidine coordination provides a stable O_2–adduct complex, Bioconj. Chem. 13 (2002) 397–402.
[13] (a) E. Tsuchida, T. Komatsu, K. Hamamatsu, Y. Matsukawa, A. Tajima, A. Yoshizu, Y. Izumi, K. Kobayashi, Exchange transfusion of albumin–heme as an artificial O_2-infusion into anesthetized rats: physiological responses, O_2-delivery and reduction of the oxidized hemin sites by red blood cells, Bioconj. Chem. 11 (2000) 46–50;
(b) Y. Huang, T. Komatsu, A. Nakagawa, E. Tsuchida, S. Kobayashi, Compatibility in vitro of albumin–heme (O_2-carrier) with blood cell components, J. Biomed. Mater. Res. 66A (2003) 292–297;
(c) E. Tsuchida, T. Komatsu, Y. Matsukawa, A. Nakagawa, H. Sakai, K. Kobayashi, M. Suematsu, Human serum albumin incorporating synthetic heme: red blood cell substitute without hypertension by nitric oxide scavenging, J. Biomed. Mater. Res. 64A (2003) 257–261.
[14] E. Tsuchida, T. Komatsu, K. Arai, H. Nishide, Synthesis and O_2-binding properties of tetraphenylporphyrinatoiron(II) derivatives bearing a proximal imidazole covalently bound at the β-pyrrolic position, J. Chem. Soc., Perkin Trans. 2 1995 (1995) 747–753.
[15] B.T. Doumas, W.A. Watson, H.G. Biggs, Albumin standards and measurement of serum albumin with bromcresol green, Clin. Chim. Acta 31 (1971) 87–96.
[16] H. Watanabe, K. Yamasaki, U. Kragh-Hansen, S. Tanase, K. Harada, A. Suenaga, M. Otagiri, In vivo and in vitro properties of recombinant human serum albumin from *Pichia pastoris* purified by a method of short processing time, Pharm. Res. 18 (2001) 1775–1781.
[17] J.P. Collman, J.I. Brauman, B.L. Iverson, J.L. Sessler, R.M. Morris, Q.H. Gibson, O_2 and CO Binding to iron(II) porphyrins: a comparison of the "picket fence" and "pocket" porphyrins, J. Am. Chem. Soc. 105 (1983) 3052–3064.
[18] T.G. Traylor, S. Tsuchiya, D. Campbell, M. Mitchell, D. Stynes, N. Koga, Anthracene heme cyclophanes: steric effects in CO, O_2, and RNC binding, J. Am. Chem. Soc. 107 (1985) 604–614.
[19] E. Tsuchida, T. Komatsu, K. Arai, H. Nishide, Synthesis and dioxygen-binding properties of double-sided porphyrinatoiron(II) complexes bearing covalently bound axial imidazole, J. Chem. Soc., Dalton Trans. 1993 (1993) 2465–2469.
[20] E. Katchalski, G.S. Benjamin, V. Gross, The availability of the disulfide bonds of human and bovine serum albumin and of bovine g-globulin to reduction by thioglycolic acid, J. Am. Chem. Soc. 79 (1957) 4096–4099.

[21] D.R. Grassetti, J.F. Murray Jr., Determination of sulfhydryl groups with 2,2′ - or 4,4′ -dithiopyridine, Arch. Biochem. Biophys. 119 (1967) 41–49.
[22] A.O. Pedersen, J. Jacobsen, Reactivity of the thiol group in human and bovine albumin at pH 3–9, as measured by exchange with 2,2′ - dithiodipyridine, Eur. J. Biochem. 106 (1980) 291–295.
[23] E.J. Cohn, The properties and functions of the plasma proteins, with a consideration of the methods for their separation and purification, Chem. Rev. 28 (1941) 395–417.
[24] I. Sjöholm, I. Ljungstedt, Studies on the tryptophan and drug-binding properties of human serum albumin fragments by affinity chromatography and circular dichroism measurements, J. Biol. Chem. 248 (1973) 8434–8441.
[25] A. Sumi, W. Ohtani, K. Kobayashi, T. Ohmura, K. Yokoyama, N. Nishida, T. Suyama, Purification and physicochemical properties of recombinant human serum albumin, in: C. Rivat, J.-F. Stoltz (Eds.), Biotechnology of Blood Proteins, vol. 227, John Libbey Eurotext, Montrouge, 1993, pp. 293–298.
[26] S. Gumpen, P.O. Hegg, H. Martens, Thermal stability of fatty acid–serum albumin complexes studies by differential scanning calorimetry, Biochim. Biophys. Acta 574 (1979) 189–196.
[27] T. Kosa, M. Maruyama, M. Otagiri, Species differences of serum albumins: II. Chemical and thermal stability, Pharm. Res. 15 (1998) 449–454.
[28] a G. Sudlow, D.J. Birkett, D.N. Wade, The Characterization of two specific drug binding sites on human serum albumin, Mol. Pharmacol. 11 (1975) 824–832;
b G. Sudlow, D.J. Birkett, D.N. Wade, Further characterization of specific drug binding sites on human serum albumin, Mol. Pharmacol. 12 (1976) 1052–1061.
[29] G. Scatchard, A.C. Batchelder, A. Brown, Chemical, clinical, and immunological studies on the products of human plasma fractionation: VI. The osmotic pressure of plasma and of serum albumin, J. Clin. Invest. 23 (1944) 165–170.
[30] S. Sakata, M.Z. Atassi, Immunochemistry of serum albumin. X. Five major antigenic sites of human serum albumin are extrapolated from bovine albumin and confirmed by synthetic peptides, Mol. Immunol. 17 (1980) 139–142.
[31] C. Lapresle, N. Doyen, Studies of an antigenic site of human-serum albumin with monoclonal-antibodies, Mol. Immunol. 20 (1983) 549–555.
[32] W. Ohtani, Y. Nawa, K. Takeshima, H. Kamuro, K. Kobayashi, T. Ohmura, Physicochemical and immunochemical properties of recombinant human serum albumin from *Pichia pastoris*, Anal. Biochem. 256 (1998) 56–62.
[33] T.R. McCurdy, S. Gataiance, L.J. Eltringham-Smith, WP. Sheffield, A covalently linked recombinant albumin dimer is more rapidly cleared in vivo than are wild-type and mutant C34A albumin, J. Lab. Clin. Med. 143 (2004) 115–124.
[34] a J.P. Collman, J.I. Brauman, K.M. Doxsee, T.R. Halbert, E. Bunnenberg, R.E. Linder, G.N. LaMar, J.D. Guadio, G. Lang, K. Spartalian, Synthesis and characterization of "tailed picket fence" porphyrins, J. Am. Chem. Soc. 102 (1980) 4182–4192;
b J.P. Collman, F. Basolo, E. Bunnenberg, T.C. Collins, J.H. Dawson, P.E. Ellis Jr., M.L. Marrocco, A. Moscowitz, J.L. Sessler, T. Szymanski, Use of magnetic circular dichroism to determine axial ligation for some sterically encumbered iron(II) porphyrin complexes, J. Am. Chem. Soc. 103 (1981) 5636–5648;
c J.P. Collman, J.I. Brauman, T.J. Collins, B.L. Iverson, G. Lang, R.B. Pettman, J.L. Sessler, M.A. Walters, Synthesis and characterization of the "pocket" porphyrins, J. Am. Chem. Soc. 105 (1983) 3038–3052.
[35] J. Geibel, J. Cannon, D. Campbell, T.G. Traylor, Model compounds for R-state and T-state hemoglobins, J. Am. Chem. Soc. 100 (1978) 3575–3585.
[36] C.A. Sawicki, Q.H. Gibson, Properties of the T state of human oxyhemoglobin studied by laser photolysis, J. Biol. Chem. Soc. 252 (1977) 7538–7547.

Functional Analysis of Recombinant Human Serum Albumin Domains for Pharmaceutical Applications

Sadaharu Matsushita,[1] Yu Isima,[1] Victor Tuan Giam Chuang,[1,2] Hiroshi Watanabe,[1] Sumio Tanase,[3] Toru Maruyama,[1] and Masaki Otagiri[1,4]

Received December 7, 2003; accepted June 10, 2004

Purpose. Functional analysis of the three recombinant human serum albumin (rHSA) domains and their potential as stand-alone proteins for use as drug delivery protein carriers.

Methods. Protein structure was examined by fluorescence and CD spectroscopy. Ligand binding was estimated by ultrafiltration. Antioxidant activity was estimated by measuring the quenching of dihydrorhodamine 123. Esterase-like activity and enolase-like activity were estimated from the rate of hydrolysis of *p*-nitrophenyl acetate and conversion of dihydrotestosterone from the 3-keto to 3-enol form, respectively. The domains of human serum albumin (HSA) were radiolabeled with ^{111}In to evaluate their pharmacokinetics.

Results. The ligand binding ability of subsites Ia and Ib could not be detected in domain II. However, the binding of ligands to subsite Ic and site II were preserved in domain II and domain III, respectively. Domain III retained about 45% of its esterase-like activity, and weaker esterase-like activity was also observed in domain I. All domains showed low enolase-like activity in a pH 7.4 phosphate buffer, but domain II had higher activity in a pH 9.2 carbonate buffer. Domain I exhibited antioxidant activity comparable to that of rHSA. All three of the ^{111}In-radiolabeled domains were rapidly eliminated from HSA, with high accumulation in the kidneys.

Conclusion. Domain I of HSA has great potential for further development as a drug delivery protein carrier, due to its favorable properties and the presence of a free cysteine residue.

KEY WORDS: antioxidant activity; domain; enzyme activity; human serum albumin; pharmacokinetics.

INTRODUCTION

Human serum albumin (HSA) is a biological macromolecule that has potential for a wide range of pharmaceutical applications. Due to its remarkably long half-life, its wide *in vivo* distribution, and its lack of substantial immunogenicity, HSA is an ideal carrier for therapeutic peptides and proteins that interact with cellular or molecular components in the vascular and interstitial compartments (1). One strategy for overcoming lack of specificity of a drug toward target tissues is to covalently couple the drug to a suitable carrier. Drug carriers should have high rates of accumulation in the target tissue, low rates of uptake by normal tissue, and low toxicity. They should be easily linked to the drug, and should readily release the drug in the target tissue. Also, they should be readily available and affordable. Several studies have shown that HSA fulfills these requirements for delivery of drugs to tumors (2,3). HSA also appears to be suitable for delivering drugs such as methotrexate to neoplastic tissue and to inflamed joints of patients with rheumatoid arthritis (4). Also, studies have shown that genetic fusion of bioactive peptides to HSA can produce therapeutic HSA derivatives with appropriate pharmacokinetic properties. Therapeutic proteins genetically fused to albumin have been found to have longer circulating half-lives and improved stability. Examples of such genetically fused proteins include interferon-rHSA (Albuferon), human growth hormone-rHSA (Albutropin), recombinant granulocyte colony stimulating factor (rG-CSF)-rHSA (Albugranin), hirudin-albumin fusion protein and serum albumin-CD4 genetic conjugate (5–8).

HSA is a monomeric non-glycosylated polypeptide with a heart-shaped structure that is approximately 67% α-helix and contains no β-sheet. It is composed of three homologous domains (I-III), and each domain has two subdomains (A and B) that possess common structural elements (1). In addition to its remarkable ligand binding properties, HSA has been shown to possess antioxidant activity, esterase-like activity and enolase-like activity (9–13). Expression of recombinant HSA (rHSA) and its recombinant domains has been reported, and the structural basis of their ligand interactions has been examined using methods including X-ray crystallography (14–16). Examination of the crystal structure of ligand-albumin complexes has revealed positions of binding sites and tertiary structure locations of reactive amino acid residues such as Cys-34, which is involved in NO conjugation (17).

Effects of intrinsic functional properties of HSA other than its ligand binding ability on its role as a drug carrier are poorly understood. There is little doubt that carrier proteins can strongly influence the magnitude of the therapeutic response to a conjugated drug. This influence is thought to be especially significant in the case of peptide drugs and drugs conjugated to a carrier protein via a peptide linker. For example, Albuferon is reportedly approximately 20 times less potent than IFN-α on a molar basis (5). Thus, detailed investigation of the influence of HSA on drugs conjugated to it is important for understanding drug targeting, modification of drug pharmacokinetics, stability of drug-albumin conjugates and, most importantly, design of more sophisticated drug delivery carrier systems. In the present study, we used *Pichia pastoris* to separately express the three recombinant domains of HSA, in order to determine the location of its active sites and clarify the mechanisms underlying its functions such as ligand binding, antioxidant activity and enzyme-like activities.

[1] Department of Biopharmaceutics, Graduate School of Pharmaceutical Sciences, Kumamoto University, 5-1 Oe-honmachi, Kumamoto 862-0973, Japan.

[2] Department of Pharmacy, Faculty of Allied Health Sciences, Universiti Kebangsaan Malaysia, Jalan Raja Muda Abdul Aziz, 50300 Kuala Lumpur, Malaysia.

[3] Department of Medical Biochemistry, Graduate School of Medical Sciences, Kumamoto University, 1-1-1 Honjo, Kumamoto 860-0811, Japan.

[4] To whom correspondence should be addressed. (e-mail: otagirim@gpo.kumamoto-u.ac.jp)

ABBREVIATIONS: DHT, 5α-dihydrotestosterone; DNSA, dansyl-L-asparagine; DNSS, dansylsarcosine; DRD, dihydrorhodamine 123; HSA, human serum albumin; rHSA, recombinant HSA; *n*-butyl *p*-AB, *n*-butyl *p*-aminobenzoate; RD, rhodamine 123; RSA, rabbit serum albumin.

MATERIALS AND METHODS

Materials

Racemic ketoprofen was a gift from the Kissei Pharmaceutical Co. (Matsumoto, Japan). The following were obtained as pure substances from the manufacturer: warfarin (Sigma, St. Louis, MO, USA), dansyl-L-asparagine (DNSA) (Sigma), dansylsarcosine (DNSS) (Sigma), dihydrorhodamine 123 (DRD) (Sigma), *n*-butyl *p*-aminobenzoate (*n*-butyl *p*-AB) (Wako, Osaka, Japan), *p*-nitrophenyl acetate (Nacalai Tesque, Kyoto, Japan), 5α-dihydrotestosterone (DHT) (Merck, Darmstadt, Germany), and tritiated (1,2) dihydrotestosterone (40 Ci/mmol) (PerkinElmer Life Sciences, Inc., Boston, MA, USA). The scintillation cocktail Hionic-fluor was purchased from Packard Co. (Meriden, CT, USA). Restriction enzymes, calf intestinal alkaline phosphatase and TaKaRa EX *Taq* DNA polymerase were obtained from Takara Shuzo Co. Ltd (Kyoto, Japan). A DNA sequence kit was obtained from Applied Biosystems (Foster City, CA, USA). The *Pichia* Expression kit was purchased from Invitrogen Corp. (Carlsbad, CA, USA). Other chemicals used were obtained from commercial suppliers.

Synthesis and Purification of rHSA and Domains

The protocol used to express and purify domains I, II, and III of HSA was a modification of a previously published protocol (14,18). The segments coding for rHSA and the individual HSA domains were amplified by the polymerase chain reaction using a cDNA clone of HSA as the template. The domains contained the following amino acids: domain I, 1-197; domain II, 187-385; domain III, 381-585. The 5′-sense primers encoded an *Xho* I restriction site. The 3′-antisense primers were designed to incorporate an *Eco* RI site, and to add a stop codon to terminate the translation. The sequences of the 5′-primers were as follows: 5′-GGACTAGTCTCGAGAAAAGAGATGCACACAAGAGTG-3′ (rHSA and domain I), 5′-GGACTAGTCTCGAGAAAAGAGATGAAGGGAAGGC-3′, (domain II), and 5′-GGACTAGTCTCGAGAAAAGAGTGGAAGAGCCTCAG-3′ (domain III). The sequences of the 3′-primers were as follows: 5′-CGCGAATTCTTATCTCTGTTTGGCAGACGAAGCC-3′ (domain I), 5′-CGCGAATTCTTACTGAGGCTCTTCCACAAGAGG-3′ (domain II), and 5′-CGCGAATTCTTATAAGCCTAAGGCAGC-3′ (rHSA and domain III). The amplified gene segments were ligated into the pPIC9 vector, which contains an α-factor secretion signal sequence. The resulting vector was introduced into the yeast species *Pichia pastoris* (strain GS115). The secreted rHSA and individual domains were isolated from the growth medium by a combination of precipitation with 60% (w/v) $(NH_4)_2SO_4$ and purification on a Blue Sepharose CL-6B column (Amersham Pharmacia Co., Uppsala, Sweden) and a TSKgel SuperQ-TOYOPEARL650 column (Tosoh Co., Tokyo, Japan). Isolated protein was defatted using the charcoal procedure described by Chen (19), deionized, freeze dried and then stored at −20°C until used. The resulting rHSA and individual domains (treated with dithiothreitol) exhibited a single band on SDS-PAGE. N-terminal amino acid sequences of the proteins were determined using a Perkin-Elmer ABI 477A protein sequencer.

Fluorescence and CD Spectra Measurements

Intrinsic fluorescence spectra were obtained using a Jasco FP-777 spectrofluorometer (Tokyo, Japan) equipped with thermostatically controlled 1-cm quartz cells and 5-nm excitation and emission bandwidths. rHSA and individual domains were excited at 295 nm, and the spectra were corrected for buffer baseline fluorescence. CD spectra were obtained using a JASCO J-720 spectropolarimeter (JASCO, Tokyo, Japan) at 25°C. Far- and near-UV CD spectra were recorded at protein concentrations of 5.0 μM and 15 μM, respectively, in 67 mM phosphate buffer (pH 7.4).

Ultrafiltration

The interaction of site I ligands (warfarin, DNSA, *n*-butyl *p*-AB) and site II ligands (ketoprofen, DNSS) with rHSA and individual domains in 67 mM phosphate buffer (pH 7.4) was examined using ultrafiltration at 25°C. An amicon MPS-1 micropartition system with a YMT ultrafiltration membrane was used. First, 1-ml samples were ultrafiltered at 2000 rpm for 40 min at 25°C. The concentration of the free drug was determined by HPLC using a system consisting of a Hitachi L-6200 Pump and an F-1050 Fluorescence Spectrophotometer or L-4000 UV Detector. LiChrosorb RP-18 (Cica Merck, Tokyo, Japan) was used as the stationary phase. The mobile phases were as follows: 30 mM phosphate buffer (pH 7.7)–acetonitrile (57.5:42.5, v/v) for warfarin, DNSA and DNSS; deionized water-acetonitrile (30:70, v/v) for *n*-butyl *p*-AB; 0.2 M acetate buffer (pH 4.5)-acetonitrile (60:40, v/v) for ketoprofen. Ketoprofen was detected at 257 nm using a UV monitor. Warfarin, DNSA, DNSS and *n*-butyl *p*-AB were detected using a fluorescence monitor. The excitation/emission wavelengths were as follows: warfarin, 300 nm/400 nm; DNSA, and DNSS, 330/550 nm; *n*-butyl *p*-AB, 290 nm/350 nm. Because we detected slight adsorption of *n*-butyl *p*-AB to the membrane and apparatus, the ultrafiltration system was siliconized by treatment with Sigmacote (Sigma, St. Louis, MO, USA) to prevent adsorption. The data were corrected using a calibration curve obtained from the concentrations of ultrafiltered ligand in the absence of protein. The adsorption of other ligands to the membrane and apparatus was negligible. The bound ligand concentration (C_b) was calculated using the following equation:

C_b = total ligand concentration (before ultrafiltration)

(C_t) − ligand concentration in filtrated fraction (C_f) (1)

The bound percentage was calculated using the following equation:

$$\frac{C_b}{C_f + C_b} \times 100 \quad (2)$$

Determination of Esterase-like Activity

The reaction of *p*-nitrophenyl acetate with rHSA and individual domains was followed spectrophotometrically at 400 nm (JASCO Ubest-35 UV-VIS spectrophotometer) by monitoring the appearance of *p*-nitrophenol. The reaction mixtures contained 5 μM *p*-nitrophenyl acetate and 20 μM protein in 67 mM phosphate buffer (pH 7.4). Reactions were followed at 25°C. Pseudo-first-order rate constant analysis

was performed, as described elsewhere (11,12), and the apparent hydrolysis rate constants (k_{obs}) were calculated.

Enolase-like Activity Assay

The final volume of the reaction mixture used in the measurement of enolase activity of rHSA and individual domains was 250 μl and contained the following: 67 mM phosphate buffer (pH 7.4) or carbonate buffer (pH 9.2), 0.4 μCi [1,2-3H] DHT (about 300,000 CPM), 20 μM radioinert DHT, and enzyme preparation. After incubation at 37°C for 90 min, 1 ml of a dextran-coated charcoal suspension (1% charcoal and 0.1% dextran [av. mol. wt. 35,000–45,000] in 67 mM phosphate buffer [pH 7.4] or carbonate buffer [pH 9.2]) was added, and the suspension was then allowed to stand for 10 min at room temperature. The suspension was then centrifuged for 5 min at 10,000 rpm. A 0.4-ml aliquot of the resulting supernatant was added to 4 ml of scintillation cocktail, and the radioactivity was determined using a LSC-5100 liquid scintillation counter (Aloka, Tokyo, Japan). Total enolase activity was subtracted from activity in the absence of protein (background). The steroid was removed by adsorption on charcoal. The counted radioactivity was due to tritiated water released from DHT, as evidenced by the following: 1) radioactivity was not measurable in the absence of protein; 2) evaporation of the reaction product (after treatment with charcoal suspension) to dryness resulted in the loss of radioactivity (13).

Reactive Oxygen Species (ROS) Quenching Capacity

H_2O_2 oxidizes DRD to rhodamine 123 (RD), which fluoresces at 536 nm when excited at 500 nm. We prepared 2-ml samples of rHSA or individual domains (7.5 μM) and DRD (5 μM) in 67 mM phosphate buffer (pH 7.4), and at predetermined times, H_2O_2 (25 mM) was added. The progress of the reactions was followed spectrophotometrically by measurement of the RD formed at 25°C by fluorescence. Controls were performed without additives. The quenching of the control was 0%.

In Vivo Experiments

Animals

Male ddY mice (6 weeks old, 25–35 g) were purchased from the Kyudou Co (Kumamoto, Japan). The animals were maintained under conventional housing conditions. The experiments were performed in accordance with the Principles of Laboratory Animal Care adopted and promulgated by the United States National Institutes of Health.

Biodistribution Experiment

rHSA and individual domains were radiolabeled with ^{111}In using DTPA anhydride, as described elsewhere (20). Each radiolabeled derivative was purified by gel-filtration chromatography using a Sephadex G-25 column with elution by a 0.1 M acetate buffer (pH 6.0). The absorbency of the eluants was measured at 280 nm, and the protein-containing fractions were pooled. The resulting solution was concentrated and washed with 0.9% NaCl by ultrafiltration. The specific activity of each derivation was approximately 37 MBq/mg protein. The mice received a 0.1 mg/kg dose of ^{111}In-rHSA conjugate in saline by injection into the tail vein. At 1, 3, 5, 10, and 30 min after injection of the ^{111}In-rHSA conjugate, blood was collected from the vena cava with the animal under ether anesthesia, and plasma was obtained by centrifugation. At each of these time points, an animal was sacrificed for excision of liver and kidney. These organs were then rinsed with saline, weighed, and examined for radioactivity. ^{111}In radioactivity was counted using a well-type NaI scintillation counter (ARC-2000; Aloka, Tokyo, Japan).

Pharmacokinetic Analysis

The tissue distribution patterns of the ^{111}In-rHSA derivatives were evaluated according to organ uptake clearance using a previously reported method (21). In the early period after injection, the efflux of ^{111}In radioactivity from the organs was assumed to be negligible, because the degradation products of ^{111}In-labeled ligands, prepared using DTPA anhydride, do not easily pass through biologic membranes (21). This assumption was supported by the fact that no ^{111}In was detected in the urine. Based on this assumption, organ uptake clearance was calculated by dividing the amount of radioactivity in an organ at 30 min by the area under the plasma concentration-time curve (AUC) at the same time point. The AUC was calculated by fitting an equation to the plasma concentrations of the derivatives using MULTI, a nonlinear least-squares program (22). Tissue distribution patterns were evaluated using tissue uptake clearance data according to the integration plot analysis. Tissue accumulation at time t was proportional to the $AUC_{0\text{-}t}$. By dividing the tissue accumulation at time t (X_t) and the $AUC_{0\text{-}t}$ by the plasma concentration (C_t), CL tissue was obtained from the slope of the plot of X_t/C_t vs. $AUC_{0\text{-}t}/C_t$. A previous report (23) has shown that ^{111}In is not suitable for evaluating the dynamic phase of a protein with a long *in vivo* half life. Therefore, we estimated the total, liver and kidney clearance within a period of 30 min.

Statistical Analysis

All data are presented as mean ± SD. Statistical analysis of differences was performed by one-way ANOVA followed by a modified Fisher's least squares difference method.

RESULTS

Structural Aspects of the Recombinant HSA Domains

Previous experiments in our laboratory demonstrated that rHSA expressed with a yeast expression system and then purified exhibited structural and functional properties that were very similar to those of HSA. The recombinant domains expressed in the present study exhibited structural properties identical to those reported by Dockal *et al.* (data not shown). Individual domains expressed in the present study were similar in length to those reported by Dockal *et al.* (14), except that domain II had 2 additional residues at the N-terminal in the present study (187-385). N-terminal amino acid sequences of the proteins expressed in the present study were consistent with the corresponding portions of native HSA. The three recombinant domains of HSA exhibited secondary and tertiary structures comparable to those of rHSA. The sum of the observed ellipticities of the three domains shows the same

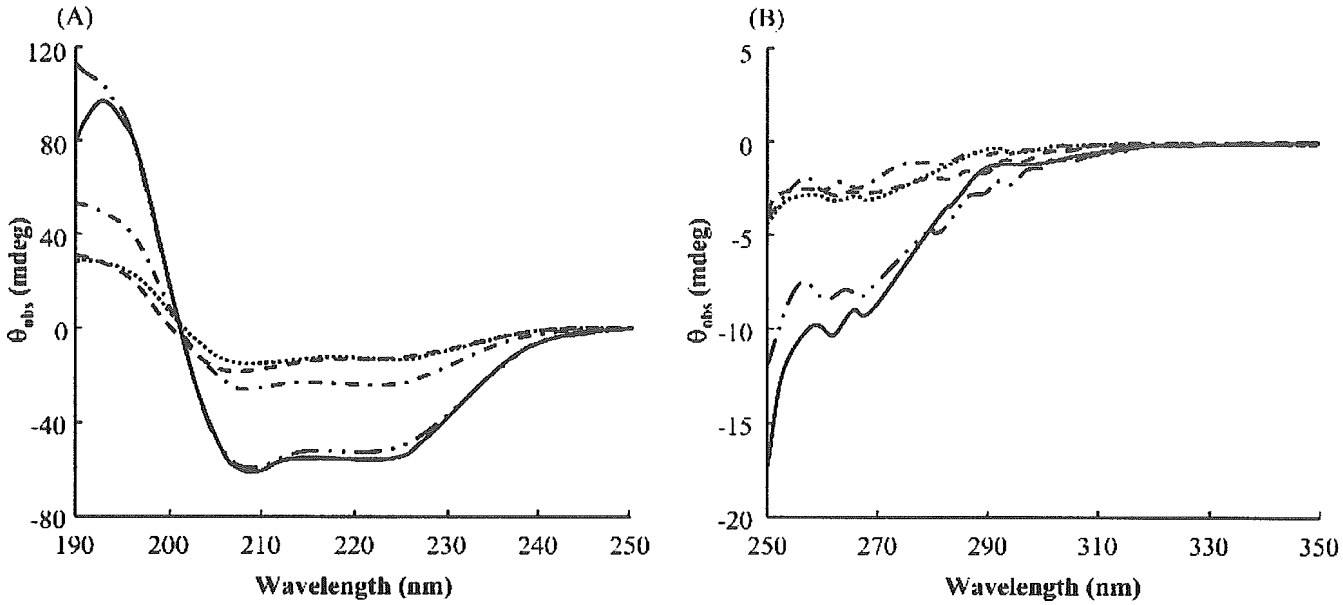

Fig. 1. Observed ellipticities of far-UV (A) and near-UV (B) CD spectra for rHSA (——), domain I (·····), domain II (----), domain III (– · – ·) and calculated signal of the three domains combined (— ·· —). Far- and near-UV CD spectra were recorded at protein concentrations of 5 μM and 15 μM, respectively, in 67 mM phosphate buffer (pH 7.4 and 25°C).

minima and shape as rHSA, especially at wavelengths above 265 nm in the near-UV CD spectra, suggesting that their conformation is similar to their native structure as constituents of rHSA (Fig. 1).

Ligand Binding Ability of the Recombinant HSA Domains

Although there have been reports of the ligand binding ability of each HSA domain, there have been no reports of the quantitative binding and ligand binding to subsites of site I. In this study, the percentage of ligand (2.5 μM) bound to rHSA and individual domains (5 μM) was determined by ultrafiltration. Table I shows the binding percentage of warfarin, DNSA and *n*-butyl *p*-AB, which are markers of subsite Ia, Ib, and Ic, respectively (24). Negligible amounts of warfarin and DNSA bound to each single domain. However, the binding percentage of *n*-butyl *p*-AB to rHSA was 50%, and a significant amount of *n*-butyl *p*-AB bound with domain II.

Table I. Binding of Warfarin, DNSA, and *n*-Butyl *p*-AB to rHSA and Individual Domains

	Percentage bound (%)		
HSA	Warfarin (Ia)	DNSA (Ib)	*n*-butyl *p*-AB (Ic)
rHSA	50.93 ± 1.94	42.36 ± 2.74	14.38 ± 5.72
Domain I	6.48 ± 0.67[a]	3.29 ± 2.96[a]	1.27 ± 0.37[a,c]
Domain II	7.46 ± 4.26[a]	2.46 ± 1.69[a]	9.39 ± 1.79[b]
Domain III	5.18 ± 2.00[a]	3.36 ± 2.94[a]	3.00 ± 1.06[b,d]

The sample solutions contained 2.5 μM warfarin, DNSA or *n*-butyl p-AB and 5 μM rHSA or individual domains in 67 mM phosphate buffer (pH 7.4 and 25°C). All values are mean ± SD (n = 3 to 5).
[a] $p < 0.01$ vs. rHSA.
[b] $p < 0.05$ vs. rHSA.
[c] $p < 0.01$ vs. domain II.
[d] $p < 0.05$ vs. domain II.

The intrinsic fluorescence spectra originating from Trp-214 shows that the relative fluorescence intensity of domain II was low and its λ_{max} was blue-shifted, compared with rHSA (Fig. 2). Table II shows the percentage of bound ketoprofen and DNSS, which are site II markers of HSA. Ketoprofen and DNSS bound to domain III with greater affinity than the site I markers to domain II, but ketoprofen and DNSS bound with greater affinity to rHSA than to domain III.

Esterase-like Activities of the Recombinant HSA Domains

The catalytic activity of rHSA and individual domains with respect to *p*-nitrophenyl acetate is shown in Table III. Esterase-like activity was detected in domain III, where site II is located (18), but this activity was about 45% of that of rHSA. Activity was also detected in domain I, although it was much lower than that of rHSA or domain III. However, no activity was detected in domain II.

Enolase-like Activities of the Recombinant HSA Domains

We used a radioisotope tracer to measure the enolase-like activity (conversion of the 3-keto form of DHT to the 3-enol form) of the HSA domains (Table IV). The enolase-like activity of HSA is influenced by pH and the type of buffer used. The activity increases with increasing pH, but at very high pH, especially over pH 11.0, enolization is a self-catalyzed reaction for compounds containing a keto group. The behavior of DHT in the present study was the same as reported previously (13). Accordingly, we examined enolase-like activity under two conditions: in a carbonate buffer at pH 9.2, conditions under which the highest activity has been observed and the self-catalyzed reaction is negligible; and in a phosphate buffer at pH 7.4, which are more typical experimental conditions. All HSA domains showed only low activity in the phosphate buffer (pH 7.4). The activity of rHSA was higher in the carbonate buffer (pH 9.2) than in the phosphate